


# Cardiac fibroblasts display endurance to ischemia, high ROS control and elevated respiration regulated by the JAK2/STAT pathway

Aida Beà<sup>1</sup>, Juan García Valero<sup>2,3</sup>, Andrea Irazoki<sup>4</sup>, Carlos Lana<sup>1</sup>, Guillermo López-Lluch<sup>5,6</sup>, Manuel Portero-Otín<sup>7</sup>, Patricia Pérez-Galán<sup>2,3</sup>, Javier Inserte<sup>8,9</sup>, Marisol Ruiz-Meana<sup>8,9</sup>, Antonio Zorzano<sup>4</sup>, Marta Llovera<sup>1</sup> and Daniel Sanchis<sup>1</sup> 

<sup>1</sup> Cell Signaling & Apoptosis Group, Institut de Recerca Biomèdica de Lleida (IRBLleida), Universitat de Lleida, Spain

<sup>2</sup> Department of Hematology-Oncology, Institut d'Investigacions Biomèdiques August Pi i Sunyer (IDIBAPS), Barcelona, Spain

<sup>3</sup> Centro de Investigación Biomédica en Red-Oncología (CIBERONC), Barcelona, Spain

<sup>4</sup> Departament de Bioquímica i Biomedicina Molecular, Facultat de Biologia, Institute for Research in Biomedicine (IRB Barcelona), Barcelona Institute of Science and Technology (BIST), Centro de Investigación Biomédica en Red Diabetes y Enfermedades Metabólicas Asociadas (CIBERDEM), Universitat de Barcelona, Spain

<sup>5</sup> Andalusian Center of Developmental Biology, Pablo de Olavide University, Sevilla, Spain

<sup>6</sup> Centro de Investigación Biomédica en Red Enfermedades Raras (CIBERER), Sevilla, Spain

<sup>7</sup> Department of Experimental Medicine, IRBLleida, University of Lleida, Lleida, Spain

<sup>8</sup> Laboratory of Experimental Cardiology, Vall d'Hebron-Institut de Recerca, Universitat Autònoma de Barcelona, Spain

<sup>9</sup> Centro de Investigación Biomédica en Red-CV (CIBER-CV), Barcelona, Spain

## Keywords

cardiac fibroblast; cellular respiration; JAK/STAT; ROS; survival

## Correspondence

M. Llovera and D. Sanchis, Cell Signaling & Apoptosis Group, Institut de Recerca Biomèdica de Lleida (IRBLleida), Universitat de Lleida, Biomedicina-I, Av. Rovira Roure, 80, 25125 Lleida, Catalonia, Spain  
 Tel: +34 973 70 29 49  
 E-mails: marta.llovera@udl.cat (ML); daniel.sanchis@udl.cat (DS)

(Received 1 September 2021, revised 9 November 2021, accepted 17 November 2021)

doi:10.1111/febs.16283

Cardiovascular diseases are the leading cause of death globally and more than four out of five cases are due to ischemic events. Cardiac fibroblasts (CF) contribute to normal heart development and function, and produce the post-ischemic scar. Here, we characterize the biochemical and functional aspects related to CF endurance to ischemia-like conditions. Expression data mining showed that cultured human CF (HCF) express more *BCL2* than pulmonary and dermal fibroblasts. In addition, gene set enrichment analysis showed overrepresentation of genes involved in the response to hypoxia and oxidative stress, respiration and Janus kinase (JAK)/Signal transducer and Activator of Transcription (STAT) signaling pathways in HCF. *BCL2* sustained survival and proliferation of cultured rat CF, which also had higher respiration capacity and reactive oxygen species (ROS) production than pulmonary and dermal fibroblasts. This was associated with higher expression of the electron transport chain (ETC) and antioxidant enzymes. CF had high phosphorylation of JAK2 and its effectors STAT3 and STAT5, and their inhibition reduced viability and respiration, impaired ROS control and reduced the expression of *BCL2*, ETC complexes and antioxidant enzymes. Together, our results identify molecular and biochemical mechanisms conferring survival advantage to experimental ischemia in CF and show their control by the JAK2/STAT signaling

## Abbreviations

AKT/PKB, protein kinase-B; CF, cardiac fibroblast; CoQ, ubiquinol/coenzyme Q; COX, cytochrome oxidase; DRP1, dynamin-related protein 1; ECM, extracellular matrix; EMT, epithelial–mesenchymal transition; ETC, electron transport chain; GSEA, gene set enrichment analysis; HCF, human cardiac fibroblast; HIF, hypoxia-inducible factor; I/R, ischemia/reperfusion; JAK, Janus Kinase; MAPK, mitogen-activated protein kinases; MFN, mitofusin; NF2L2/NRF, nuclear factor, erythroid 2 like 2; NFkB, nuclear factor kappa-B; OCR, oxygen consumption rate; OPA1, optic atrophy 1; OxPhos, oxidative phosphorylation; PGC1A, peroxisome proliferator-activated receptor gamma coactivator-1 A; RISK, reperfusion injury salvage kinase; ROS, reactive oxygen species; RRC, reserve respiration capacity; RRC, reserve respiratory capacity; SAFE, survivor activating factor enhancement; SBN, silibinin; SDH, succinate dehydrogenase; SDHA, succinate dehydrogenase subunit A; SOD2, superoxide dismutase 2; STAT, signal transducer and activator of transcription.

pathway. The presented data point to potential targets for the regulation of cardiac fibrosis and also open the possibility of a general mechanism by which somatic cells required to acutely respond to ischemia are constitutively adapted to survive it.

## Introduction

Cardiovascular diseases are the leading cause of death globally with 17.9 million deaths each year, and most of them are due to an ischemic insult (World Health Organization). Cardiac fibroblasts (CF) are involved in many aspects of heart biology including the synthesis, secretion and remodeling of the extracellular matrix (ECM) in normal conditions and after an ischemic insult [1–3]. In addition, CF also influence cardiomyocyte proliferation [4] and contribute to cardiac contraction by electrical coupling between them [5] and with cardiomyocytes [6]. Activated CF, called myofibroblasts, contribute to the formation and remodeling of the fibrotic scar as a response to ischemia and hypertrophy [7]. Despite the benefit of enhanced ECM deposition after an injury, local or diffuse interstitial scarring can lead to heart failure over time by hampering proper ventricular contraction [8] and inducing arrhythmias [9]. Therefore, the control of the synthesis and deposition of the fibrotic scar has been the focus of intense analysis, as reviewed in Refs [10,11].

Cardiac fibroblasts have attracted interest as potential targets to treat different cardiovascular pathologies [11]. Identification of the precise cell types originating myofibroblasts after an injury, and the possible potential differences in the contribution to ECM secretion has been challenging [11–14]. In recent years, the number of CF, their origin and diversity, and their response to injury have been clarified by the use of genetic lineage-tracing coupled with the detection of specific gene expression, and single-cell transcriptomics. Cardiac fibroblasts have mostly an epicardial embryonic origin [15,16] and have been estimated to be approximately 13% of the total cells in the adult mouse heart [17], and 15% in the adult human ventricle [18], although variability due to species and age cannot be discarded [19]. This resident population of CFs includes several subpopulations characterized by the expression of genes related to metabolism and cell migration in the mouse heart [20] and up to seven different CF populations have been identified by transcriptomics in the human heart [18]. During an injury, CF become activated to transform into myofibroblasts, which proliferate and secrete the ECM [21,22]. The

precise types of CF activated during cardiac injury remain to be fully resolved [20].

Cardiac fibroblast proliferation, migration, transformation into myofibroblasts and scar production after an experimental infarct and in pressure-overload-induced hypertrophy have been characterized using *in vivo* experimental models [15,21,23]. In addition, the signaling pathways involved in the response of cardiac cells to myocardial cell damage has been studied in transgenic mice permanently lacking key signaling effectors [23,24], and in cell culture models *in vitro*, as reviewed by Burke *et al.* [25]. Using these approaches, acute activation of the transforming growth factor- $\beta$ , phosphoinositide 3-kinase, G-protein-coupled receptor signaling, calcineurin, the JAK/STAT pathways and inflammation have been identified as important regulators of cardiac cell survival and fibrosis after an injury [26,27]. However, the potential existence of biological characteristics and signaling pathways making fibroblasts particularly resistant to long periods of oxygen and trophic factor deprivation has not been previously investigated.

Here, by comparing CF with pulmonary and dermal fibroblasts, we identify biochemical and functional aspects specific of CF contributing and associated with their particularly high resistance to long-lasting ischemia-like conditions and identify the JAK2/STAT signaling pathway as a main regulator of these characteristics. In addition to suggest potential molecular targets to treat heart remodeling, our results open the possibility that other cell types required to respond during ischemia are also constitutively endowed to survive in hypoxic conditions.

## Results

### Neonatal rat cardiac fibroblasts express high levels of BCL2 that are required for survival in normoxia and in experimental ischemia

Rat CFs are resistant to the induction of apoptosis [28] and survive better than pulmonary fibroblasts (LF) and dermal fibroblasts (DF) in experimental conditions of 0.2% O<sub>2</sub> in Tyrode's solution, to be identified as experimental ischemia hereafter (Fig. 1A).

Higher abundance of BCL2 in CF (Ref. [28] and Fig. 1B) was involved in their resistance to cell stress-induced cytochrome *c* translocation and caspase activation [28]. Here we show that in addition to high BCL2 expression, CF also express high BCL2L1 levels (Fig. 1B) and that BCL2 has a pro-survival role in experimental ischemia and also sustains survival and proliferation in CF during normoxia (Fig. 1C), suggesting that high BCL2 expression does not only protect mitochondrial integrity in CF [28], but also could be involved in other biological processes influencing their capacity to proliferate.

### Adult human and rat cardiac fibroblasts show a specific expression program compared with pulmonary and dermal fibroblasts

Comparison of gene expression sets in cultured adult human cardiac (HCF), pulmonary (HPF) and dermal (HDF) fibroblasts obtained from public databases confirmed higher expression of *BCL2* and *BCL2L1* in HCF, compared with HPF and HDF, at the transcript level (Fig. 1D; Fig. S1A). In addition, further analysis revealed that HCF had specific enrichment in gene sets related to myogenesis and epithelial–mesenchymal transition (EMT) (Fig. 1E), which mostly involve genes related with cardiac development and with extra cellular matrix (ECM) biology, respectively, as well as gene sets related with angiogenesis, myogenesis, heart biology and ECM components (Fig. S1B). These results confirmed the identity of human fibroblast types and validated the quality of gene set enrichment analysis (GSEA). In addition, we also found differential expression in HCF of gene sets related to apoptosis, reactive oxygen species (ROS) biology, genes induced during ischemia and genes related to oxidative phosphorylation (OxPhos) (Fig. 1E; Figs S1B and S2A). Analysis of protein expression in adult rat fibroblasts showed higher expression of BCL2 and BCL2L1, relatively higher level of the ROS detoxifying enzyme superoxide dismutase-2 (SOD2) and higher abundance of the electron transport chain (ETC) complex members succinate dehydrogenase subunit A (SDHA) and cytochrome oxidase (COX) component COX4I1 in CF compared with PF and DF (Fig. 1F; Figs S1C and S2B). GSEA showed statistically significant changes in the OxPhos gene set with both up- and down-regulated components in HCF at the transcript level (Fig. 1E; Fig. S2A). A closer analysis of the OxPhos gene set showed high variability in the expression levels of key ETC complex subunits at the transcript level in human fibroblasts (Fig. S2C). Despite inherent limitations, protein and transcript expression results match with the relevant role of BCL2 in rat

neonatal CF survival and suggested potential differences among the three types of fibroblasts at the functional level in ROS detoxification and mitochondrial respiration.

### Rat cardiac fibroblasts express high levels of both ROS and ROS detoxifying enzymes and better control experimental ischemia-induced ROS than other fibroblast types

Reactive oxygen species play relevant physiological and pathological roles, contributing to the control of proliferation, differentiation and death in the cardiovascular system [29–31]. In addition, ROS production increases during hypoxia and ischemia/reperfusion (I/R) [32,33]. Because we found enrichment in genes involved in ROS biology in HCF compared with other fibroblast types (Fig. 1E and Fig. S1B), we decided to investigate the potential differences in ROS biology in CF. Our data showed that neonatal rat CF have higher expression of antioxidant enzymes SOD2, catalase and glutathione peroxidase (Fig. 2A) and higher basal concentration of mitochondrial ROS than PF and DF (Fig. 2B), but keep ROS abundance more stable in experimental ischemia than the rest of fibroblast types, in which ROS increased several folds (Fig. 2B). In summary, rat CF show high ROS abundance and better control of ROS levels during ischemia associated with higher concentration of reduced glutathione (GSH) in normal conditions (Fig. 2C).

### Rat cardiac fibroblasts have higher expression of ETC complexes II to V and higher respiration rate than other types of fibroblasts

Mitochondrial ETC activity is one of the most important sources of cellular ROS [34]. In addition, we found altered expression of genes related to oxidative phosphorylation in HCF (Fig. 1E; Fig. S2A,C) and adult rat CF (Fig. 1F; Fig. S2B). Therefore, we analyzed respiration and ETC expression in neonatal rat CF compared with PF and DF. Analysis of respiration showed that at a relative [O<sub>2</sub>] of 21%, CF had higher oxygen consumption rate (OCR) than PF and DF (Fig. 3A), with higher routine OCR, higher ATP-linked respiration, higher reserve respiratory capacity (RRC) and lower net routine control ratio, which is an indicator of the efficiency in coupling respiration to ATP synthesis, than PF and DF (Fig. 3B). Several parameters were also higher at a relative [O<sub>2</sub>] of 3% (Fig. S3A,B), which is closer to the actual tissue oxygen pressure [35,36]. The RRC has been shown to be due to ETC complex II activity and it is associated

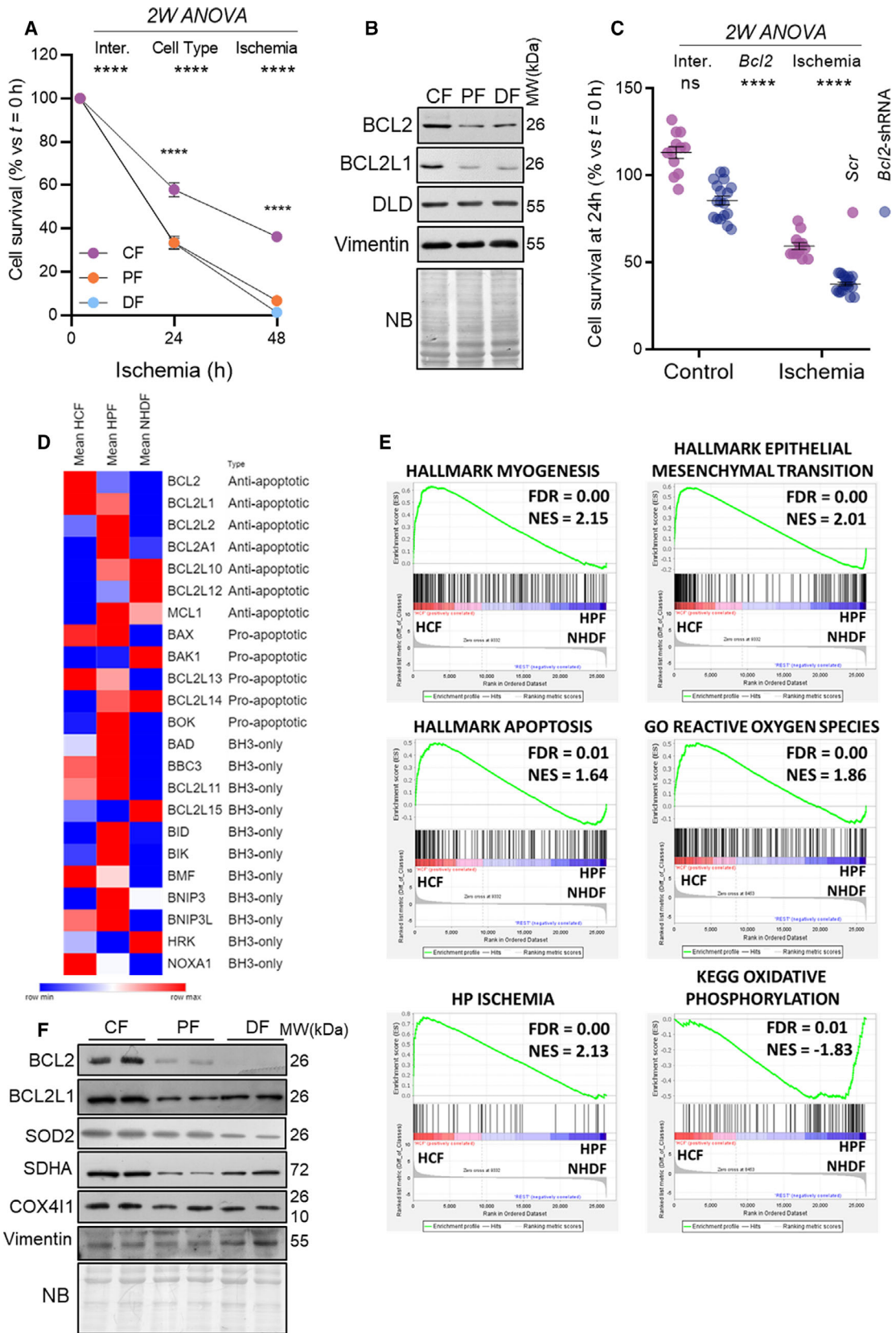




**Fig. 1.** BCL2-dependent survival to experimental ischemia of CFs compared with pulmonary and dermal fibroblasts and differential expression of genes related to relevant cellular functions in human and rat fibroblasts. (A) Survival to pO<sub>2</sub> of 0.2% in Tyrode's solution (experimental ischemia) in neonatal rat cardiac, pulmonary and dermal fibroblasts (CF, PF, DF); mean ± SEM, *N* = 15. (B) Expression of BCL2 and BCL2L1 in neonatal rat fibroblasts (DLD: dihydrolipoyl dehydrogenase, mitochondrial marker; Vimentin: fibroblast enrichment and loading marker; NB: naphthol blue membrane staining). (C) Effect of *Bcl2* gene silencing in neonatal rat CF survival in normoxia and experimental ischemia. Individual measurements, mean ± SEM, *N* = 12. (D) Heat map of the expression of *BCL2*-related genes in cultured adult HCF (*N* = 4), pulmonary fibroblasts (HPF; *N* = 5) and dermal fibroblasts (NHDF; *N* = 7). (E) GSEA plots from HCF compared with HPF and NHDF. The leading edge of each gene set, FDR (false discovery rate) and NES (normalized enrichment score) values are displayed. (F) Expression of proteins related to apoptosis, respiration and ROS control in adult rat cardiac (CF), pulmonary (PF) and dermal (DF) fibroblasts. *N* = 3. Inter, interaction; MW, molecular weight. Ns, not significant; \**P* < 0.05; \*\**P* < 0.01; \*\*\**P* < 0.001 and \*\*\*\**P* < 0.0001.

with improved resistance of cardiomyocytes to I/R [37]. We found that addition of complex II inhibitor 3-nitropropionic acid reduced the RRC confirming the important contribution of complex II to RRC in fibroblasts (Fig. S3C,D). Our results also showed that neonatal CF express higher levels of ETC complex II, III, IV and ATP synthase (complex V), yet they have similar expression of ETC complex I, Cytochrome *c* and other mitochondrial membrane and mitochondrial matrix proteins compared with PF and DF (Fig. 3C and Fig. S3E). Ubiquinol/Coenzyme Q (CoQ) abundance and redox state was similar in all the fibroblast types, although there was a tendency of CF to have more oxidized CoQ<sub>9</sub>, but not CoQ<sub>10</sub> (Fig. 3D). Despite

the differences in the expression of the ETC complexes, mitochondrial mass was similar in the three fibroblast types (Fig. 3E). Because BCL2 is highly expressed in CF and has been reported to regulate respiration under some conditions [38,39], we sought to determine the possible role of BCL2 in the regulation of RRC in neonatal CF by downregulating its expression. However, in the conditions tested, reduced *Bcl2* expression did not affect basal OCR nor RRC in CF (Fig. S4A,B). Taken together, these results showed that CF have higher ROS abundance associated with higher oxygen consumption, higher expression of ETC complexes-II-V in a similar amount of mitochondria than other types of fibroblasts, indicating that these cells have profound

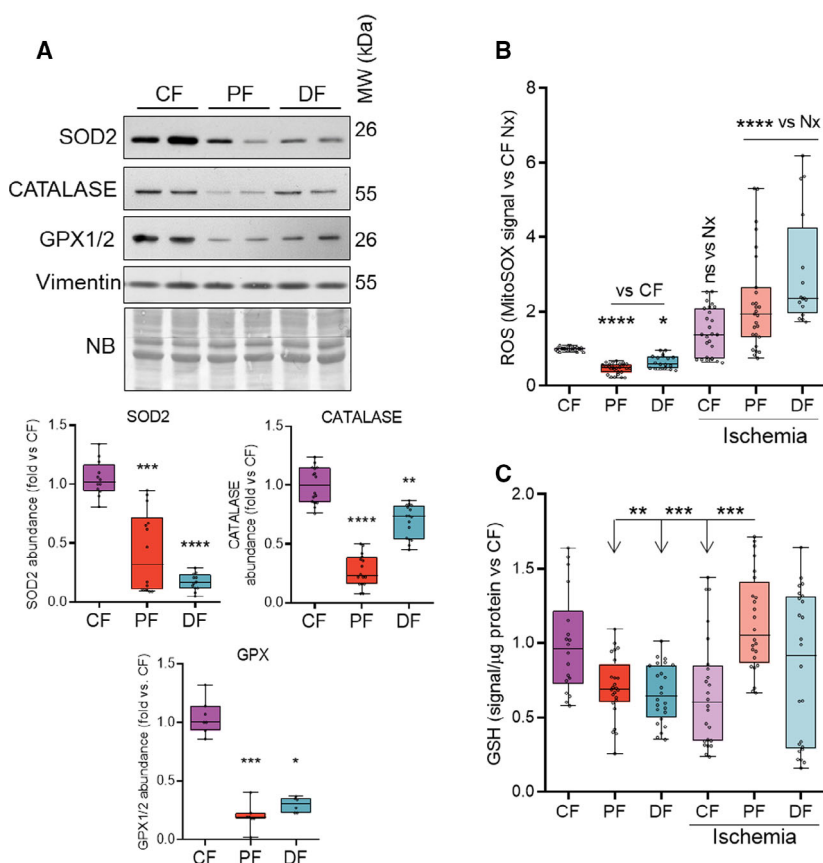


**Fig. 2.** Rat neonatal CFs have high expression of antioxidant enzymes and high basal ROS production yet enhanced ROS control in experimental ischemia. (A) Expression of antioxidant enzymes in cardiac (CF), pulmonary (PF) and dermal fibroblasts (DF). Individual relative expression values. *N* = 3 in duplicates per fibroblast type. (B) ROS in normoxia and after 24 h of experimental ischemia referred to the mean of control CF in the same experiment. *N* = 13 in duplicates. (C) Reduced glutathione quantitation on samples described in B. Graphs show individual experimental values, interquartile ranges, median and min/max. Kruskal–Wallis test was performed followed by Dunnett's or Dunn's test. Ns, not significant; \**P* < 0.05; \*\**P* < 0.01; \*\*\**P* < 0.001 and \*\*\*\**P* < 0.0001.

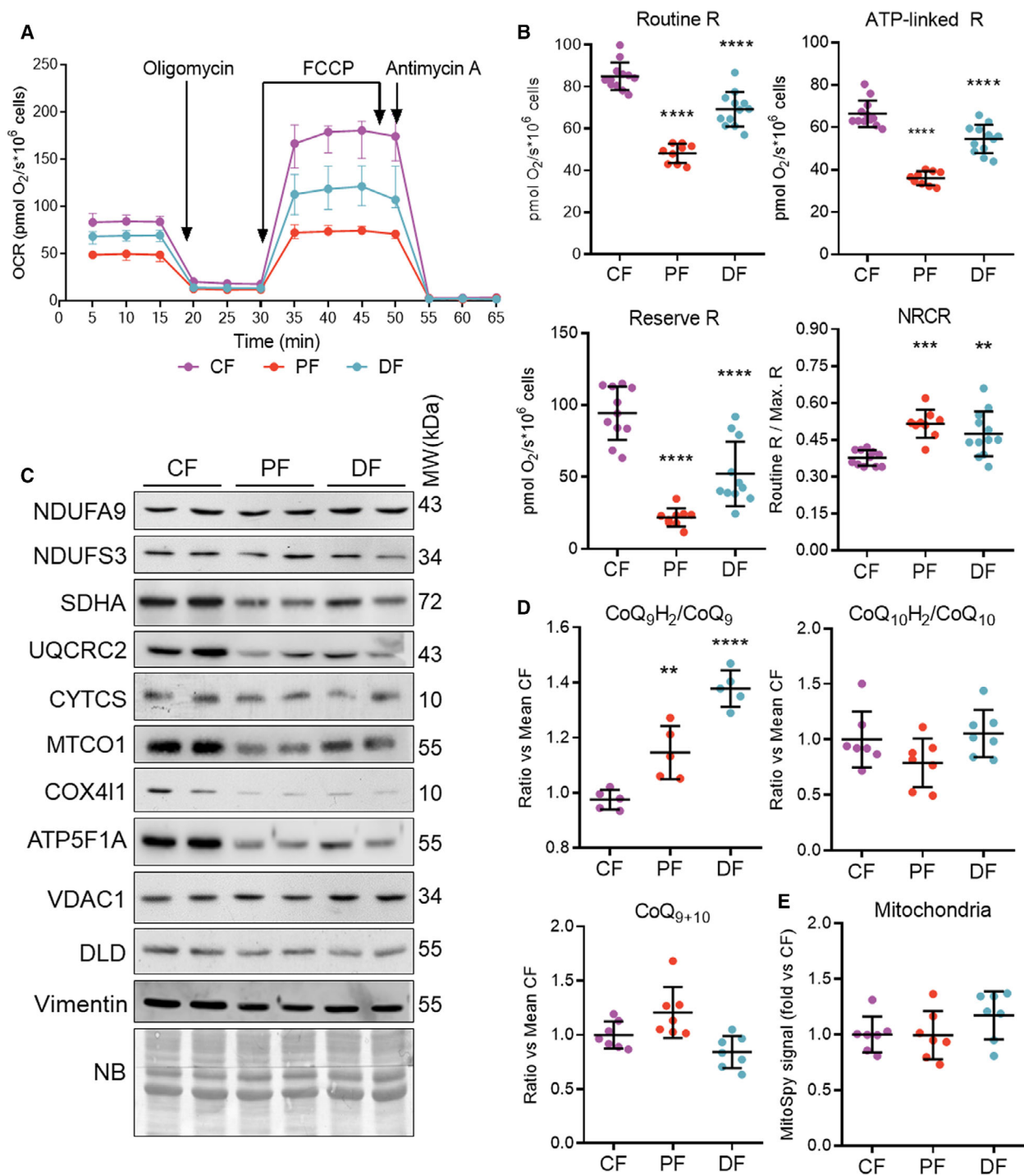


**Fig. 3.** Rat neonatal CFs have high respiration rate and high expression of ETC complexes. (A) OCR of cultures of neonatal rat cardiac (CF), pulmonary (PF) and dermal (DF) fibroblasts in basal conditions and in the presence of the complex V inhibitor oligomycin, the uncoupler FCCP and the complex III inhibitor antimycin A, allowing to calculate the different components contributing to oxygen consumption. Mean  $\pm$  SEM,  $N = 13$  in duplicates. (B) Routine (basal), ATP-linked and reserve respiration rates as well as NetRoutine Ratio (NRCR), which expresses ADP phosphorylation-related respiration as a fraction of the electron transfer capacity. (C) Expression of ETC proteins, mitochondrial markers and vimentin: (fibroblast enrichment and loading marker). Representative blots of  $N = 5$  independent with two independent plates per condition. MW, molecular weight. Densitometry shown in Fig. S3E. (D) CoQ abundance and redox status;  $N = 6$ . (E) MitoSpy mitochondrial probe signal as an indication of the total mitochondrial content;  $N = 7$ . Individual experimental data, means  $\pm$  SD. One-way ANOVA and Bonferroni's test for multiple comparisons between fibroblast types against CF was performed. Ns, not significant; \* $P < 0.05$ ; \*\* $P < 0.01$ ; \*\*\* $P < 0.001$  and \*\*\*\* $P < 0.0001$ .

adaptations in terms of mitochondrial biology, respiratory capacity and ROS metabolism.

### **Rat cardiac fibroblasts display a more fragmented mitochondrial network than pulmonary or dermal fibroblasts**

The expression of ETC complexes, the control of oxygen consumption and the rate of ROS production is orchestrated by genes governing mitochondrial dynamics, the organized process of mitochondrial fusion and fission, allowing cells to adapt to fluctuating energy demands/availability and cell stress [40–42]. Therefore, we checked the expression of several regulators of mitochondrial dynamics. Optic Atrophy 1 (OPA1) and Dynamin-related Protein 1 (DRP1) were expressed at similar amounts in all types of fibroblasts (Fig. 4A). On the contrary, expression of Mitofusin 1 (MFN1), and specially, Mitofusin 2 (MFN2), which are required for mitochondrial fusion, was lower in CF (Fig. 4A and Fig. S5). Low MFN expression was associated with lower expression of PPARC coactivator 1 alpha (PGC1A), a master regulator of mitochondrial biogenesis [43], which controls MFN expression [44] (Fig. 4A and Fig. S5). Confocal microscopy of mitochondria-labeled fibroblasts showed that rat CF have a more fragmented mitochondrial network than pulmonary and dermal fibroblasts (Fig. 4B).

Mitochondrial network fragmentation has been associated with several cellular contexts with reduced ETC activity and low mitochondrial membrane potential ( $\Delta\Psi_m$ ) [41], yet on the opposite, hormonal activation of mitochondrial fission in brown adipocytes is required for enhanced respiration associated with thermogenesis [45]. In CF, we found that in addition to high ETC activity (Fig. 3A), they had higher  $\Delta\Psi_m$  than PF and DF (Fig. 4C) and increased ROS production in the presence of rotenone, which inhibits electron transport from complex I to CoQ (Fig. 4D). This effect has been found when electrons exit directly from complex I [42,46,47]. Therefore, our results showed that improved survival of CF is associated with low MFN expression and a more fragmented mitochondrial network than other fibroblast types. Nevertheless, CF have higher expression of ETC complexes II–V, higher respiration rate and RRC, high  $\Delta\Psi_m$  and high ROS production and superior control of ROS under ischemic conditions than other fibroblast types.

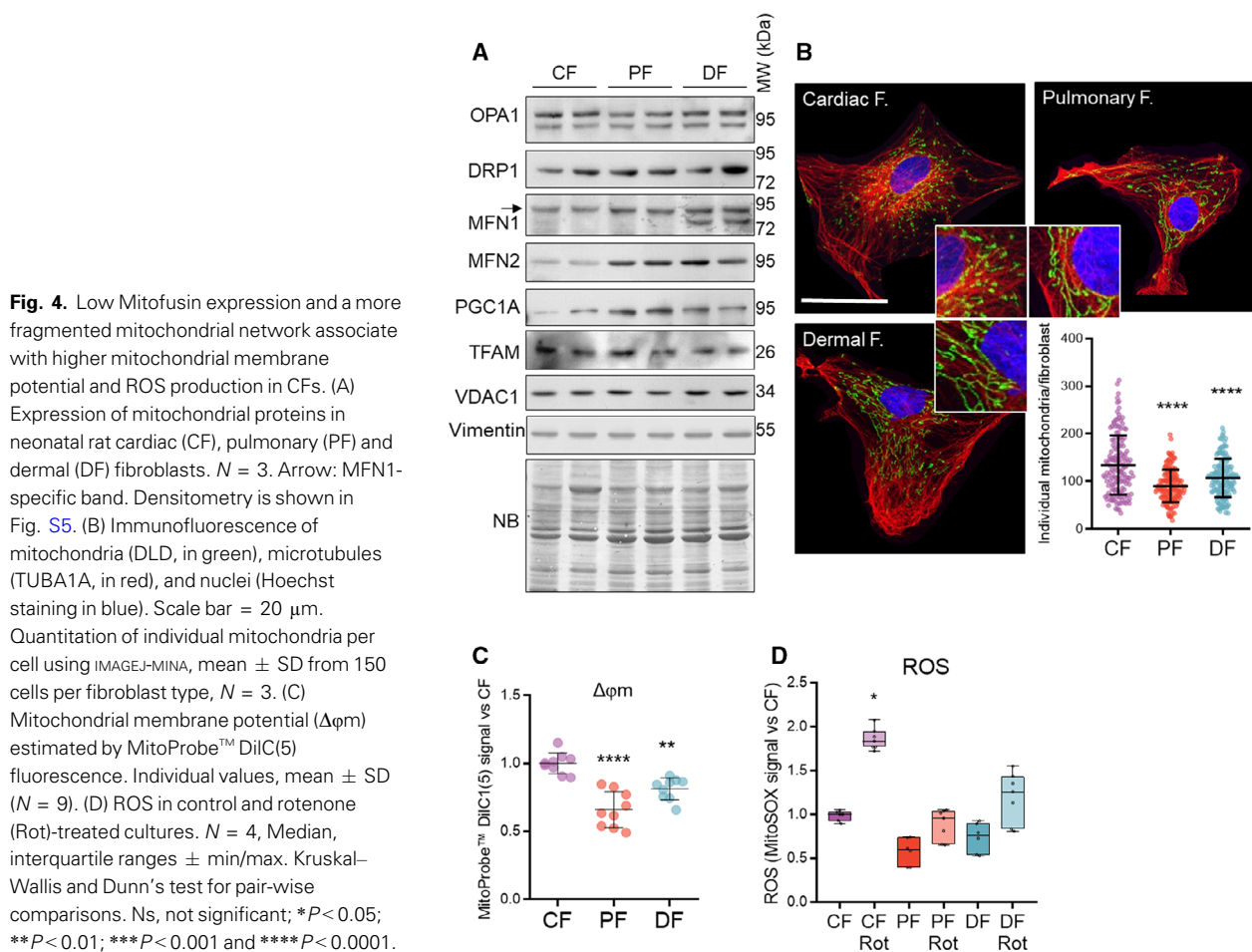
### **Status of the main pro-survival signal transduction pathways in cardiac fibroblasts**

Next, we wanted to identify the signal transduction pathways involved in the regulation of the functional

and molecular differential characteristics of CF. The activities of AKT/PKB, and the mitogen-activated protein kinases (MAPK) ERK1 and ERK2, are involved in the *reperfusion injury salvage kinase* (RISK) pathway [27]. However, our results did not support a relevant role of the RISK pathway in the survival advantage of CF, compared with PF and DF (Fig. S6A–C). The potential implication of hypoxia inducible Factor 1 subunit alpha (HIF1A), nuclear factor, erythroid 2 like 2 (NF2L2 /NRF2) and RELA/p65 from the NFKB pathway, was also assessed due to their pro-survival roles in response to changes in the oxygen pressure, ROS abundance and ischemia [48–52]. However, in the conditions tested, expression and location of key members of these pathways were not significantly different among the three fibroblast types (Fig. S6D–G). Therefore, we set to analyze alternative signaling pathways differentially enhanced in CF.

### **Constitutive activation of STAT3 and STAT5 regulates survival in cardiac fibroblasts and maintain some of their molecular and functional characteristics**

The transcription factor STAT3 is a key component of the *Survivor Activating Factor Enhancement* (SAFE) pathway, which is involved in cardiomyocyte protection during ischemia-reperfusion injury [53]. In addition, STAT3 has been suggested to activate *Bcl2* expression [54–59], to stimulate mitochondrial respiration [60–62] and to limit ROS abundance by inducing *Sod2* expression [63,64]. The *in silico* analysis of gene expression of human adult fibroblasts showed enrichment in gene sets related to STATs signaling in CF (Fig. S7). Neonatal CFs had higher p-Tyr705-STAT3 levels than PF and DF, indicating higher activation (Fig. 5A). We also assessed the abundance of p-Tyr705-STAT3 and vimentin in adult rat heart and lung histologic samples. The results showed increased phosphorylation of STAT3 related to vimentin expression in the heart compared with the lung (Fig. S8A). Then, we assessed the effect of STAT3 inhibition in CF survival in basal and ischemic conditions. We used Silibinin (SBN), a flavonolignan, which has been shown to inhibit STAT3 phosphorylation and to hamper its binding to DNA [65]. Addition of SBN to the culture medium decreased p-Tyr705-STAT3 and STAT3 total protein in a time and dose-dependent manner in CF (Fig. S8B). The presence of SBN reduced the survival of CF in normoxia and in experimental ischemia (Fig. 5B), and induced a reduction in the expression of BCL2L1 and SDHA, and a moderate



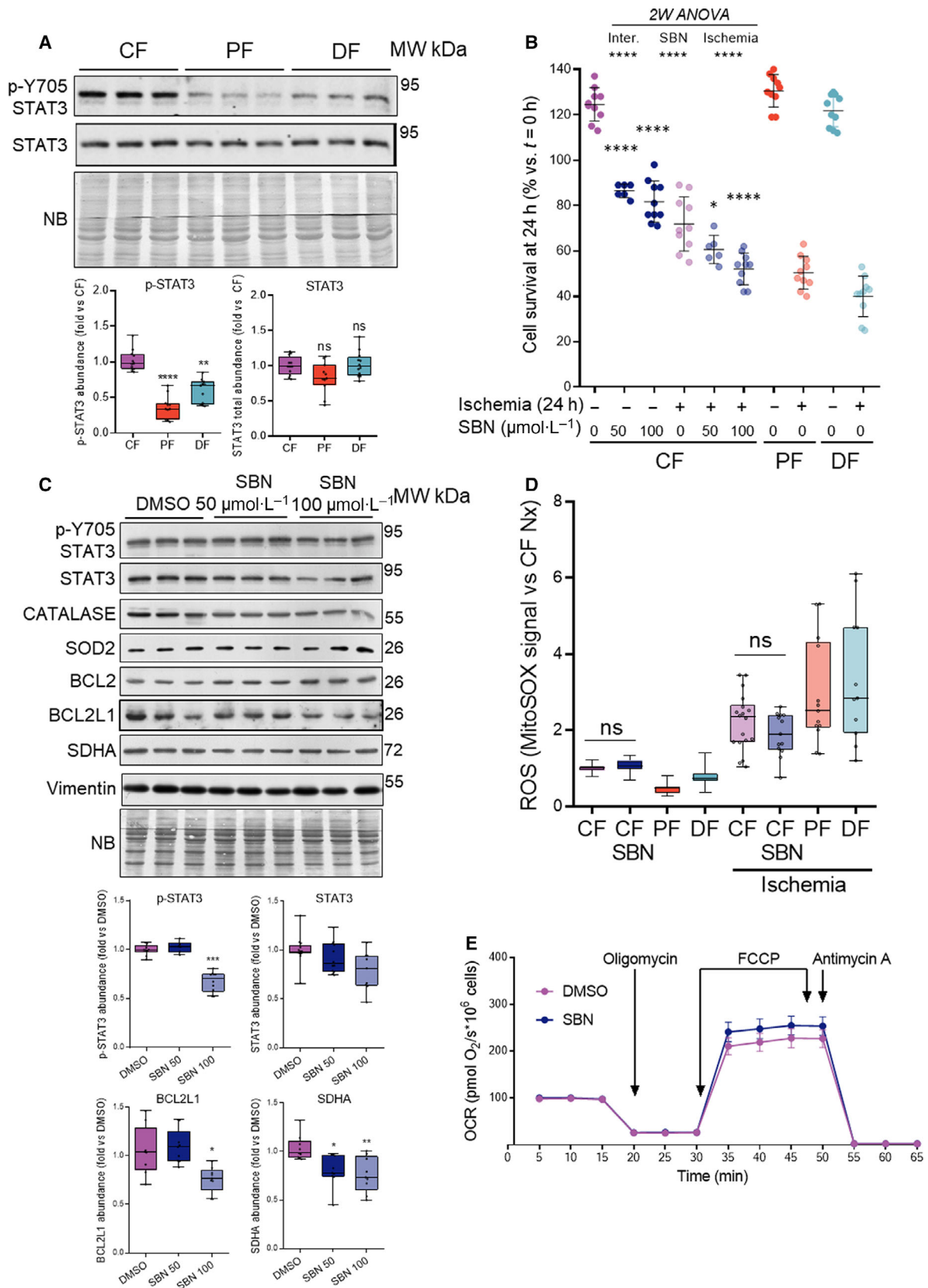
reduction of catalase expression (Fig. 5C). Total STAT3 protein was reduced after SBN treatment, probably due to an autoregulation of transcription that is blocked by SBN. No effects were observed neither on the control of ROS (Fig. 5D) nor on cellular respiration at 24 h (Fig. 5E, Fig. S8C) and 48 h of SBN treatment (Fig. S8D). Interestingly, SBN did not affect survival/proliferation of PF and DF in normoxia and only induced a slight decrease of survival in DF during experimental ischemia *in vitro* (Fig. S8E). These

results suggested that STAT3 is highly activated in CF and plays a relevant function in CF survival, but showed that it is not important for the control of respiration and for the expression of BCL2 and SOD2 in CF, contrary to what has been described in other models [54,55,57,60,64].

We found enrichment of the STAT5-related gene set in adult human CF (Fig. S7). In addition, CFs had higher p-Tyr694-STAT5A levels than PF and DF (Fig. 6A). Addition of the specific STAT5 inhibitor

**Fig. 5.** High basal activation of STAT3 in rat CFs determines their survival advantage in experimental ischemia and expression of BCL2L1. (A) Basal total and phosphorylated STAT3 in neonatal rat cardiac (CF), pulmonary (PF) and dermal (DF) fibroblasts.  $N = 4$ . Individual values, interquartile ranges, median and min/max. Kruskal–Wallis and Dunn’s test against CF. (B) Survival of CF treated with the STAT3 inhibitor Silibinin (SBN). Survival of pulmonary (PF) and dermal (DF) fibroblasts is included as a reference. Experimental values, mean  $\pm$  SD,  $N = 5$ . Two-way ANOVA and Tukey’s test were performed. Identified are differences against vehicle (DMSO)-treated CF. (C) Protein expression in control (DMSO) and SBN-treated CF for 24 h.  $N = 4$ . Individual values, median, interquartile ranges and min/max. Kruskal–Wallis and Dunnett’s test were performed. (D) ROS in DMSO-treated cardiac, dermal and pulmonary fibroblasts (CF, PF, DF) and SBN-treated CF in normoxia and 24 h ischemia.  $N = 5$ . Kruskal–Wallis and Dunn’s test. (E) OCR of CF cultures treated with DMSO or SBN  $100 \mu\text{mol}\cdot\text{L}^{-1}$  for 24 h. Components contributing to OCR are shown in Fig. S8C. Mean  $\pm$  SEM,  $N = 7$ . Ns, not significant; \* $P < 0.05$ ; \*\* $P < 0.01$ ; \*\*\* $P < 0.001$  and \*\*\*\* $P < 0.0001$ .





AC-4-130 reduced the survival of CF in normoxia and in experimental ischemia, to levels of PF and DF (Fig. 6B), yet did not affect the survival of PF and DF in normoxia and only slightly affected the DF survival during experimental ischemia *in vitro* (Fig. S9A). STAT5 inhibition reduced the expression of BCL2, without significantly affecting the expression of the rest of the proteins assessed (Fig. 6C; Fig. S9B). Addition of AC-4-130 did not affect respiration nor ROS production in CF (Fig. S9C,D). Co-treatment with both STAT3 and STAT5 inhibitors reduced the CF survival at levels similar to those attained by the treatment with a single inhibitor (Fig. 6D) and slightly affected the viability of PF and DF without achieving statistical significance, except for ischemic DF (Fig. S9E). The STATs inhibitor cocktail induced downregulation of BCL2, and to a lesser extent, BCL2L1 (Fig. 6E; Fig. S9F), without affecting respiration or ROS production (Fig. S9G,H). Together, these results showed that STAT3 and STAT5 were more active in CF and were involved in the control of survival and the expression of pro-survival proteins BCL2 and BCL2L1. However, they were not relevant regulators of respiration and ROS production.

### JAK2 is constitutively activated and required for the regulation of survival, ROS production and respiration in cardiac fibroblasts

The kinase JAK2 is an upstream regulator of STAT3, STAT5 [66] and other STAT proteins as previously reviewed [67]. Therefore, we assessed the basal levels of JAK2 Tyr-1007 phosphorylation in the three fibroblast types. Cardiac fibroblasts showed the highest basal levels of p-JAK2 (Fig. 7A). Treatment with the JAK2-specific inhibitor Tyrphostin AG490 [68] induced a reduction in CF survival (Fig. 7B) similar to that attained by treatments with SBN and AC-4-130, yet affected only slightly the survival of PF and DF (Fig. S10A). Interestingly, and contrary to the inhibition of STAT3 and STAT5, AG490 also reduced CF respiration (Fig. 7C), specially affecting the reserve

respiration capacity (Fig. S10B). Furthermore, JAK2 inhibition induced an increase in ROS production in CF (Fig. 7D). These events occurred with a decrease in the expression of ETC complexes and antioxidant enzymes, except catalase (Fig. 7E; Fig. S10C).

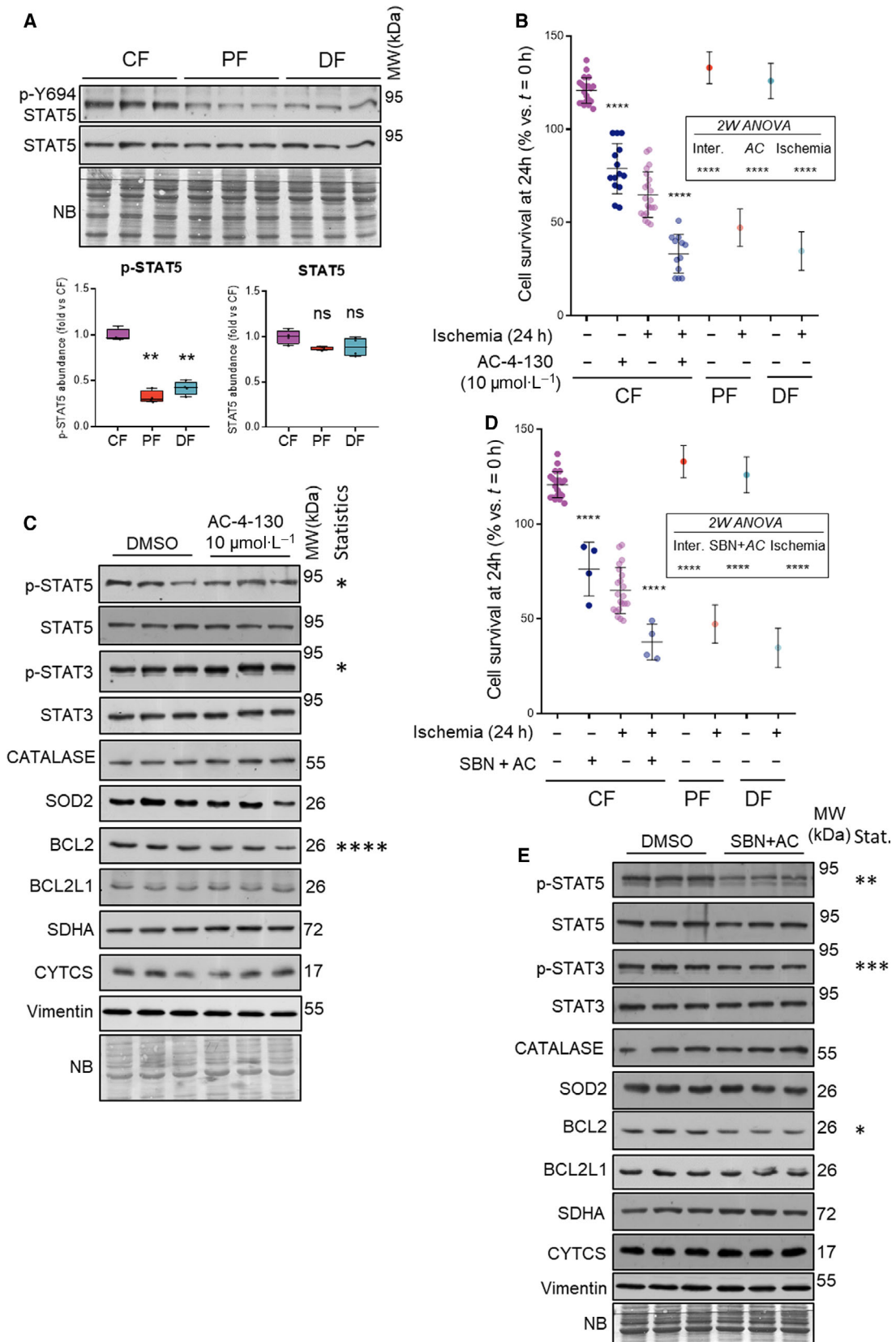
Together, these results showed that inhibition of JAK2 nullified almost all the functional traits and molecular characteristics associated with the survival advantage of CF, while inhibition of STAT3, STAT5 or combined inhibition of both did so only partially, suggesting that JAK2 uses additional mechanisms, besides STAT3 and STAT5, to control most of the characteristics endowing CF with their specific pro-survival traits.

## Discussion

The present study demonstrates that rat CF have a set of biochemical and functional characteristics associated with improved survival during long-lasting *in vitro* ischemia-like conditions (oxygen, nutrient and growth factor deprivation in uncontrolled pH), which are regulated by high constitutive activation of the JAK2/STAT signaling pathway. We found that in addition to high expression of anti-apoptotic BCL2, CF also express high levels of BCL2L1, ROS detoxifying enzymes and ETC complexes II–V, together with high ROS production and a better ROS control during long-term experimental ischemia, high respiration rates and a more fragmented mitochondrial network than other fibroblasts. Our results also show that human CF exhibit a gene expression pattern suggesting that they are endowed with the differential characteristics found in rat CF.

Recent contributions have shed light on key aspects of CF such as their actual abundance [17], functions [15,69], genetic identity [13], as well as on myofibroblast origin and transformation [15], and the cell types contributing to ECM deposition [21,23]. Together, this new information highlights the essential role of resident CF during heart function and healing. The new data have improved the understanding of the response

**Fig. 6.** High STAT5 activation in rat CFs contributes to their survival advantage during *in vitro* experimental ischemia and to high BCL2 expression. (A) Total and phosphorylated STAT5 in neonatal rat cardiac (CF), pulmonary (PF) and dermal (DF) fibroblasts.  $N = 3$ . Individual values, interquartile ranges, median and min/max. Kruskal–Wallis test followed by Dunn's test against CF. (B) Effect of STAT5 inhibition (AC-4-130 at  $10 \mu\text{mol}\cdot\text{L}^{-1}$ ) in survival. PF and DF values are included as a reference (same than in Fig. 5B). Individual values, mean  $\pm$  SD.  $N = 10$ . Two-way ANOVA and Tukey's test were performed. Shown are differences against vehicle (DMSO)-treated CF. (C) Protein expression in control CF (DMSO, vehicle) and AC-4-130-treated CF.  $N = 4$ . Kruskal–Wallis and Dunnett's tests were performed. Densitometry is shown in Fig. S9B. (D) CF survival after inhibition of STAT3 and STAT5 by SBN  $100 \mu\text{mol}\cdot\text{L}^{-1}$  and AC-4-130  $10 \mu\text{mol}\cdot\text{L}^{-1}$ . PF and DF values are same data than in Fig. 5B.  $N = 10$ . Individual values, mean  $\pm$  SD. Two-way ANOVA and Tukey's tests were performed. (E) Protein expression in control and (SBN+AC)-treated CF,  $N = 4$ . Kruskal–Wallis and Dunnett's tests were performed. Densitometry is shown in Fig. S9F. *Ns*, not significant; \* $P < 0.05$ ; \*\* $P < 0.01$ ; \*\*\* $P < 0.001$  and \*\*\*\* $P < 0.0001$ .



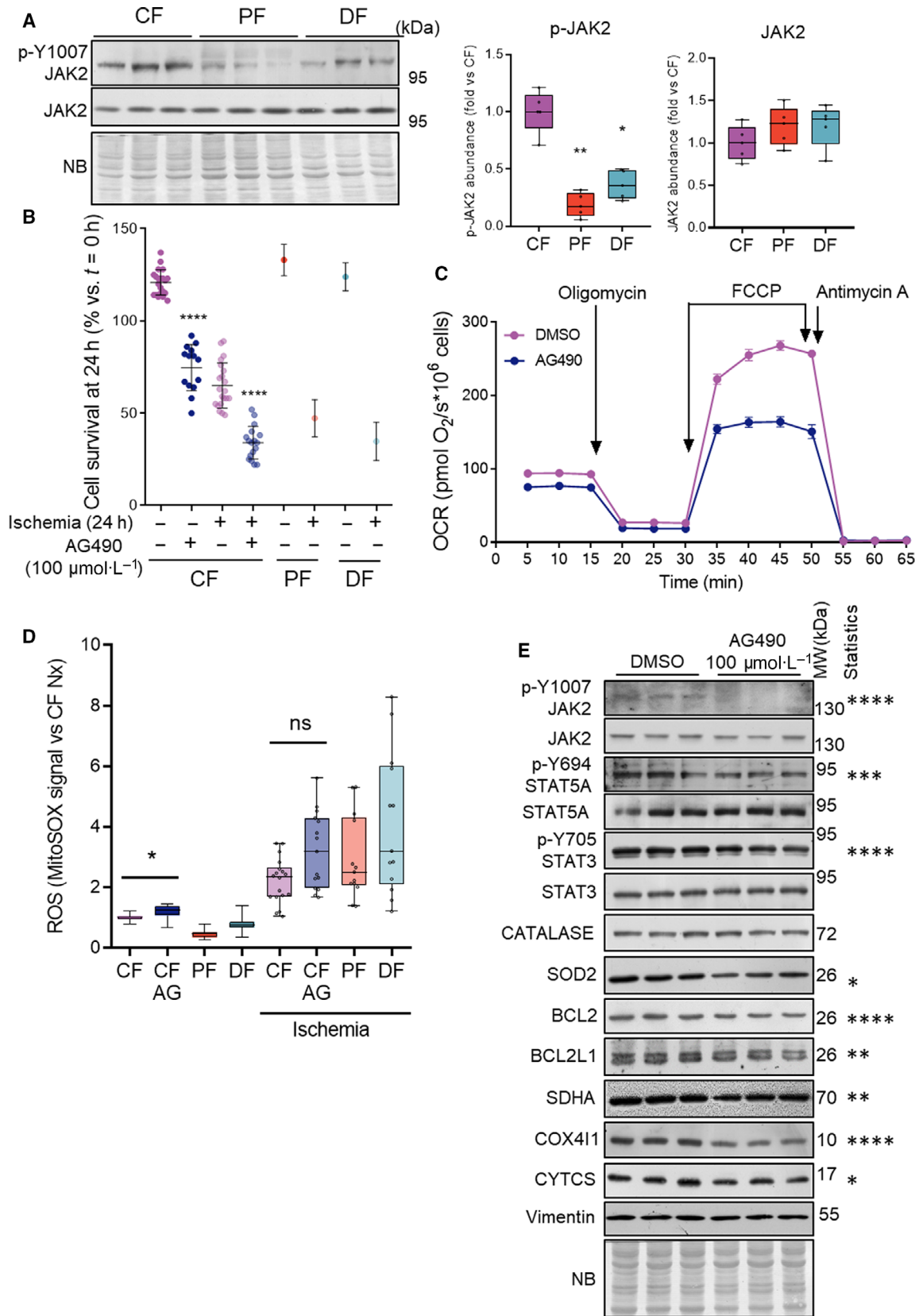




**Fig. 7.** JAK2 inhibition reverts most of the traits related to survival, respiration and ROS production of CFs. (A) Expression of total and phosphorylated JAK2 in cultures of neonatal rat cardiac (CF), pulmonary (PF) and dermal (DF) fibroblasts,  $N = 4$ . Individual values, interquartile ranges, median and min/max. Kruskal–Wallis and Dunnett’s test. (B) Survival of CF after JAK2 inhibition by AG490 at  $100 \mu\text{mol}\cdot\text{L}^{-1}$  in normoxia and experimental ischemia. PF and DF data of Fig. 5B. Mean  $\pm$  SD,  $N = 10$ . Two-way ANOVA and Tukey’s test were performed. (C) OCR of CF cultures treated with DMSO or AG490  $100 \mu\text{mol}\cdot\text{L}^{-1}$  for 24 h. Components contributing to OCR are shown in Fig. S10B. Mean  $\pm$  SEM,  $N = 7$ . (D) ROS in cells treated with AG490  $100 \mu\text{mol}\cdot\text{L}^{-1}$ . Individual experimental values, interquartile ranges, median and min/max,  $N = 14$ . Kruskal–Wallis and Dunn’s tests were performed. (E) Protein expression in control and AG460-treated CF. Kruskal–Wallis and Dunnett’s test;  $N = 4$ . Densitometry is shown in Fig. S10C. Ns, not significant; \* $P < 0.05$ ; \*\* $P < 0.01$ ; \*\*\* $P < 0.001$  and \*\*\*\* $P < 0.0001$ .

of cardiac tissue to stress and could allow the design of new therapies to control cardiac fibrosis for the treatment of adverse remodeling. However, there is less information available about the fundamental biological characteristics of CF.

### Cardiac fibroblasts display specific characteristics related to mitochondrial organization and function associated with their improved survival to ischemia compared with other fibroblasts

We previously found that rat CF express higher levels of *BCL2* than other fibroblast types and that this is associated with reduced ischemia-induced apoptosis *in vitro* [28]. Here, we expand the knowledge about the relevance of *BCL2* in CF showing that its expression regulates viability of CF in experimental ischemia and in normal conditions. Then, we addressed the question whether our findings in rat CF were also true for human CF. The analysis of gene expression arrays available in public databases confirmed a trend to higher expression of *BCL2* and *BCL2L1* in cultured human CF compared with other fibroblast types (PF and DF). In addition, GSEA of the selected human microarray expression data indicated changes in gene sets related to EMT, angiogenesis, ROS biology, oxidative phosphorylation and cell signaling in human CF compared with PF and DF. We decided to assess some of them in rat CF at the protein and functional levels, as they had never been shown before and they could have potential relevance for the understanding of CF biology and their enhanced survival to ischemia.

Our data showed that CF produce higher basal levels of mitochondrial ROS than other fibroblasts, yet kept their concentration better controlled during long-term ischemia *in vitro*. This was associated with higher constitutive expression of the ROS detoxifying enzymes SOD2, Catalase and GPX1/2. In the myocardium, ROS are involved in the control of cardiomyocyte proliferation [29] and hypertrophy [31,70]. High but controlled production of ROS in CF could contribute to their physiological and healing functions rather than to their improved survival, as we show

here that STAT inhibition abrogated CF survival in experimental ischemia without increasing the production of ROS.

Our findings on respiration demonstrate that CF have higher OCRs compared with other fibroblasts, even at an oxygen pressure of 3%, which mimics the one occurring in living tissues [35,36]. This trait had never been described before in CF and again coincides with the metabolic characteristics of some solid cancers adapted to thrive under hypoxic conditions [71]. High respiration rate and high phosphorylation efficiency in CF could help them to survive and be metabolically active at low oxygen pressure during chronic hypoxia/ischemia and during scar formation after an infarct. Our results show that ETC complex II function is required for the reserve or spared respiration, as in cardiomyocytes [37]. Our data also suggest that metabolic adaptations in CF could foster their survival during an acute blood flow shortage without the requirement of activating any additional mechanisms.

Mitochondrial dynamics contribute to the adaptation of cells to the fluctuation of ambient factors such as nutrient and oxygen availability [40,41] and are involved in processes influencing proliferation, differentiation [72], mitophagy and cell death [41,73]. Our results showed that the mitochondrial network of CF is more fragmented than that of other fibroblast types, with more individual mitochondria. This was accompanied by a higher respiration rate and  $\Delta\phi\text{m}$ . Although fragmentation of the mitochondrial network has been observed in pathological conditions associated with cell death [40] or accompanied by low oxygen consumption and decreased  $\Delta\phi\text{m}$  [41], this has been found in experimental models after genetic manipulation of key genes involved in mitochondrial dynamics [74] and, therefore, representing more challenging conditions. At the level found in CF, mitochondrial fragmentation is compatible with high oxygen respiration rate, high  $\Delta\phi\text{m}$  and improved survival, compared with PF and DF. The fragmented mitochondrial network was associated with lower expression of MFNs, MFN1 and MFN2, which are required for mitochondrial fusion [74], and the

upstream regulator PGC1A [44], in CF compared with PF and DF. Low MFN expression could participate in maintaining the fragmentation of the mitochondrial network, but also in conferring their increased resistance to cell death, as it has been observed in *Mfn2*-deficient MEFs during endoplasmic reticulum stress [75] and in *Mfn2*-deficient cardiomyocytes [76,77].

### **The JAK/STAT signaling pathway is a key regulator of survival, ROS metabolism and respiration in cardiac fibroblasts**

Our experimental data do not support a relevant role of the RISK, HIF1A and NRF2 pathways in the maintenance of CF characteristics. Increased abundance of RELA/p65 in the nuclear fraction of CF under basal and ischemic conditions compared with PF and DF is suggestive of sustained stimulation of the NF $\kappa$ B pathway, which has been shown to be induced by ROS [51].

STAT signaling has been shown to be involved in cardioprotection [53], in the control of NF $\kappa$ B activity [78], in the induction of *Bcl2* expression [54–59], in the stimulation of mitochondrial respiration [60–62] and in the inhibition of ROS production by inducing SOD2 expression [63,64]. We found enrichment in the STATs gene sets in human fibroblasts and high constitutive activation of JAK2, STAT3 and STAT5 in rat CF. Treatment of rat CF with inhibitors of the JAK2/STAT pathway abrogated most of the biochemical and functional characteristics associated with improved survival. These findings pinpoint the JAK/STAT pathway as a potential target for intervening the process of fibrosis in the heart. In addition, our data show that STAT3 controls BCL2L1 expression but not BCL2, and STAT5 controls BCL2 expression but not that of BCL2L1 in CF and that both STAT proteins contribute to maintain survival advantage of CF under control and ischemia-like conditions. Our data also indicate that high basal ROS production, improved ROS control during *in vitro* experimental ischemia and high respiration are associated with survival advantage but they are independent events. Finally, we found that only JAK2-specific inhibition abrogated ROS control and reduced the respiration. These results suggest that JAK2 interacts with additional downstream regulators and/or that it directly functions in the nucleus. In this regard, there are debated evidences of the direct role of JAK2 in the nucleus [79,80], and also reports of the interaction of JAK2 with other members of the STAT family or different adaptor proteins [67]. Completing the knowledge about the JAK2-dependent signaling in CF could be useful to design improved treatments against adverse fibrosis in the heart.

Limitations of the present study include that functional analysis have been performed in neonatal rat cells *in vitro*, which can differ from adult cells. However, in an attempt to validate some of the results, we confirmed the expression changes in adult rat cells, which are more difficult to obtain and maintain at the required number to perform functional assays. In addition, our analysis of STAT3 phosphorylation in adult rat samples suggested that STAT3 is more activated in the heart than in the lung when normalized against vimentin signal. Although rat cells could be significantly different from human cells, we found changes at the transcriptional level in cultured human adult CFs suggesting that they are also different from other fibroblast types regarding the characteristics and the signaling studied here. In addition, the *in vitro* nature of the study did not take into account factors that can influence the outcome of *in vivo* by the interaction of CF with additional cell types and factors, among other differences.

Taken together, the results presented here contribute relevant information on functions involved in key aspects of CF biology, such as endurance to experimental ischemia, ROS production and respiration, and help to understand the signaling involved in their regulation. We show that CF have enhanced the expression of anti-apoptotic proteins BCL2 and BCL2L1, antioxidant enzymes and ETC complex II–V, higher ROS production and increased respiration compared with PF and DF, and demonstrate their regulation through the JAK2/STAT signal transduction pathway. These data have potential translational implications for the management of cardiac remodeling in pathological processes involving fibrosis. In addition, our results show how a cell type required to respond to acute ischemia is constitutively adapted to low oxygen pressure conditions, broadening the potential impact of the presented findings.

## **Materials and methods**

### **Cell cultures and treatments**

The investigation with experimental animals was approved by the Experimental Animal Ethic Committee of the University of Lleida and conforms to the Guide for the Care and Use of Laboratory Animals, 8th Edition, published in 2011 by the US National Institutes of Health and EU-directive 2021/63/EU and are in compliance with the ARRIVE guidelines. Rat (*Rattus norvegicus*) neonatal fibroblasts were obtained from 3 to 4-day-old Sprague-Dawley pups (euthanasia was performed by decapitation) and cultured as previously described [28]. Adult rat fibroblasts were obtained from 3- to 4-month-old Sprague-Dawley rats. Animals were deeply anesthetized in a CO<sub>2</sub>

chamber and their hearts quickly removed. Fibroblasts were maintained in Dulbecco's Modified Eagle Medium (DMEM; Gibco; 41965-039) containing 10% FBS (Gibco, Waltham, MA, USA; 10270098), penicillin/streptomycin (Gibco; 15140-122), 0.1 mmol·L<sup>-1</sup> MEM non-essential amino acids (Gibco; 11140-035) and 1 mmol·L<sup>-1</sup> sodium pyruvate (Gibco; 11360-39) at 37 °C and 5% CO<sub>2</sub> atmosphere. Experimental ischemia-like conditions were achieved by culturing cells in Tyrode's solution (NaCl 137 mmol·L<sup>-1</sup>, KCl 2.7 mmol·L<sup>-1</sup>, Na<sub>2</sub>HPO<sub>4</sub> 8 mmol·L<sup>-1</sup>, KH<sub>2</sub>PO<sub>4</sub> 1.5 mmol·L<sup>-1</sup>, CaCl<sub>2</sub> 0.9 mmol·L<sup>-1</sup> and MgCl<sub>2</sub> 0.5 mmol·L<sup>-1</sup>) inside a hypoxic chamber (H35 Hypoxystation; Don Whitley Scientific, Bingley, UK) continuously monitored for achieving 0.2% O<sub>2</sub> and 5% CO<sub>2</sub>, and incubated at 37 °C for the time periods indicated in the figures. Silibinin (Sigma, St. Louis, MO, USA; S0417), AC-4-130 (Quimigen, Madrid, Spain; AOB36422-5), and Tyrphostin AG490 (Sigma; T3434) stock solutions were prepared in DMSO. Adult fibroblasts were isolated similarly to neonatal rats and cultured. Cell survival was quantified using the Trypan Blue exclusion assay at the end of treatments [81].

### ***In silico* gene expression analysis in human cultured fibroblasts**

mRNA relative expression levels of BCL2 family members in cultured healthy human CFs (HCF; *n* = 4), pulmonary fibroblasts (HPF; *n* = 5) and normal dermal fibroblasts (NHDF; *n* = 7) was compared according to GEP public databases (GSE136039, GSE129164, GSE89715, GSE104618 and GSE108511). These selected data were all generated with [HTA-2\_0] Affymetrix Human Transcriptome Array 2.0. Raw data were normalized to RMA using EXPRESSION CONSOLE software v1.4.1.46 (Affymetrix, Thermo Fisher Scientific, Waltham, MA, USA). To take into consideration the batch effect, joined data were normalized using the Limma package included in Transcriptome Analysis console (Applied Biosystems, Waltham, MA, USA).

Gene signatures were determined with GSEA version 4.1.0 (Broad Institute, Cambridge, MA, USA) using the hallmark gene sets, the C2 curated gene sets, the C5 gene ontology gene sets, the C6 oncogenic signatures (Molecular Signature Database v7.4). A two-class analysis with 1000 permutations of gene sets and a weighted metric were used. Expression heatmaps of BCL2 family, myogenesis, EMT, apoptosis, ROS, ischemia and oxidative phosphorylation genes were created using MORPHEUS software (<https://software.broadinstitute.org/morpheus/>, Broad Institute).

### **shRNA-induced gene silencing by lentiviral transduction**

Lentiviral-based vectors for RNA interference-mediated gene silencing were pLKO.1-puro from Sigma-Aldrich, St.

Louis, MO, USA: shRNAs scrambled (SHC001), a cocktail of shRNAs of *Bcl2* [TRCN0000004679 (1), TRCN0000004680 (2), TRCN0000006261 (3)], of *Nfe2l2* [TRCN0000012132 (1), TRCN0000012128 (2), TRCN0000012129 (3), TRCN0000054659 (4), TRCN0000054662 (5)]. Lentiviral particles were produced in Human Embryonic Kidney 293 cells (HEK293T) as previously described [82,83]. Fibroblasts were transduced with lentiviral particles for 18 h and then, medium was replaced to allow the knockdown for 3 days. Silencing efficiency was checked by western blot in each experiment.

### **Detection of reactive oxygen species**

Reactive oxygen species production was determined by using the fluorescent probe MitoSOX™ Red (Thermo Fisher Scientific; M36008), as previously described [31]. Rat neonatal fibroblasts were washed twice in PBS, trypsinized and counted using a Neubauer cell chamber. Equal amount of cells from each population were incubated in PBS containing 2.5 μmol·L<sup>-1</sup> MitoSOX™ Red for 10 min in the dark prior to ROS measurement. The fluorescence of the cell population is proportional to the levels of intracellular ROS generated and measured with a BD FACSCanto II cytometer (Becton Dickinson, Mountain View, CA, USA) using 488 nm laser excitation and detection with BP 530/30 filter. Fluorescence values varied between days, and therefore, before statistical comparisons, the full set of data for each experiment was normalized to the mean value obtained the same day for CFs under normoxic conditions when indicated, Rotenone (Sigma; R8875) was added at 1 μmol·L<sup>-1</sup> 15 min before the analysis of ROS.

### **Quantification of GSH levels**

GSH levels were determined by using the fluorescent probe ThiolTracker™ (ThermoFisher; T10095) following the manufacturer's instructions. The ThiolTracker™ signal was normalized to the total protein concentration in the plate (μg).

### **Determination of mitochondrial abundance and mitochondrial membrane potential**

Abundance of mitochondria was estimated by using the fluorescent probe MitoSpy™ Green FM (BioLegend, San Diego, CA, USA; 424805) and the mitochondrial membrane potential was determined using MitoProbe™ DiIC1 (5) (ThermoFisher; M34151) following the manufacturer's instructions. Briefly, fibroblasts were washed twice in PBS, trypsinized and counted using Neubauer cell chamber. Equal amounts of cells from each population were incubated in PBS containing 250 nmol·L<sup>-1</sup> MitoSpy™ or 50 nmol·L<sup>-1</sup> MitoProbe™ for 30 min in the dark. Next, cells were washed with PBS and analyzed through flow

cytometry with BD FACSCanto II cytometer (Becton Dickinson, Mountain View, CA, USA) using 488 nm laser excitation and detection with BP 530/30 filter for MitoS-py™, or 633 nm laser excitation and detection with BP 660/20 filter for MitoProbe™. Fluorescence values varied between days; therefore, before statistical comparisons, the full set of data for each experiment was normalized to the mean value obtained the same day for CFs in normoxic conditions.

### High-resolution respirometry

Mitochondrial respiration of neonatal fibroblasts was determined by high-resolution respirometry with Oxygraph-2k (Oroboros Instruments, Innsbruck, Austria) at 37 °C and pO<sub>2</sub> of 21% and 3%. First, calibration of oxygen concentration in the medium at air saturation was performed. During the calibration, fibroblasts were trypsinized and counted using Neubauer cell chamber to add equal amount of cells from each population. Once calibrated, the medium was aspirated and fibroblasts were transferred to the oxygraph chambers at a final density of 400 000 cells/chamber. When the oxygen flux signal was stable (routine respiration), Oligomycin (2 µg·mL<sup>-1</sup>) (complex V inhibitor) was injected until a stable steady-state signal of oxygen flux was achieved (leak respiration). Afterwards, titration with FCCP (uncoupler) was injected stepwise (0.5 µmol·L<sup>-1</sup> per injection) until oxygen signal reached a maximal level and started declining. Then, antimycin A (2.5 µmol·L<sup>-1</sup>) (complex III inhibitor) was injected to assess the non-mitochondrial respiration rate, and was subtracted from all results. All data were recorded using DATLAB software 5.2 (Oroboros Instruments). ATP-linked respiration was calculated by subtracting the leak respiration from routine respiration. RRC was calculated by subtracting routine respiration from maximal respiratory capacity. NetRoutine Ratio (Routine respiration/Leak respiration – Maximal Capacity) expresses ADP phosphorylation-related respiration as a fraction of the electron transfer capacity. 3-nitropropionic acid (Sigma-Aldrich; N5636) was added to the culture medium 1 h before mitochondrial respiration determination.

### Coenzyme-Q quantification

Total CoQ determination was performed in primary fibroblasts as previously described [84,85] by adding sodium dodecyl sulfate (1%) in PBS to cell pellets. One hundred pmol of CoQ<sub>6</sub> was added as internal control to check the extraction procedure. Ethanol : isopropanol (95 : 5) in a proportion 2 : 1 was added and mixed again during 1 min. Organic extraction was performed with hexane. After centrifugation, the upper organic phase was removed, dried, dissolved in ethanol and injected in duplicate in a Beckman 166-126 HPLC system (Beckman Coulter, Brea, CA, USA)

equipped with a 20 µL loop and a 15-cm Kromasil C-18 column (Sigma-Aldrich). Total levels of CoQ were detected by an electrochemical detector. For redox ratio between CoQ reduced/oxidized, cells were homogenized in potassium phosphate buffer. To 91.5 µL of sample, 3.5 µL mercaptoethanol and 5 µL internal standard were added to avoid oxidation and control extraction. Determination of the CoQH<sub>2</sub>/CoQ was performed using the electrochemical detector. Data are from seven independent samples of each fibroblast type.

### Protein extraction and western blotting

Protein expression was analyzed in total protein extracts from cell cultures and subcellular fractions diluted in Tris-buffered 2% SDS solution at pH 6.8, SDS/PAGE and western blots were performed as reported [82,83,86]. Primary antibodies used in this work were: Caspase 3 (#9662S, 1 : 2000), p-Tyr705-STAT3 (#9145, 1 : 2000), p-Ser473-AKT (#4060, 1 : 1000), p-Ser21/9-GSK3A/B (#9331, 1 : 1000) from Cell Signaling Technology, Danvers, MA, USA; Catalase (sc-271803, 1 : 1000), SOD2 (sc-133134, 1 : 1000), glutathione peroxidase 1/2 (GPX, sc-133160, 1 : 1000), RELA/p65 (sc-372, 1 : 1000), AKT (sc-1618, 1 : 1000) from Santa Cruz Biotechnology, Dallas, TX, USA; Cytochrome *c* (CYCS, ab110325, 1 : 2000), dihydrolipoamide dehydrogenase (DLD, ab133551, 1 : 5000), GSK3B (ab18893; 1 : 1000), mitochondrial transcription factor A (TFAM, ab131607, 1 : 1000), Mitofusin-1 (MFN1, ab126575), Porin (VDAC1, ab15895, 1 : 5000), STAT3 (ab68153, 1 : 2000), hypoxia-inducible factor 1 subunit alpha (HIF1A, ab179483, 1 : 1000), Vimentin (ab45939, 1 : 1000), nuclear factor, erythroid 2 like 2 (NF2L2/NRF2, ab137550, 1 : 1000) from Abcam, Cambridge, UK; succinate dehydrogenase subunit alpha (SDHA, A11142, 1 : 2000), ubiquinol-cytochrome *c* reductase core protein 2 (UQCRC2, A11143, 1 : 1000), Cytochrome *c* oxidase subunit 4 isoform 1 (COX4I1, A21348, 1 : 1000), ATP synthase subunit A (ATP5F1A, A21350, 1 : 1000) from Molecular Probes, Eugene, OR, USA; BCL2 (610538, 1 : 500), OPA1 (612606, 1 : 1000), DRP1 (611112, 1 : 1000), mitogen-activated protein kinase 1/3 (p41 MAPK ERK2/p44 MAPK, ERK1, 610123, 1 : 1000) from BD Biosciences, Franklin Lakes, NJ, USA; NADH:ubiquinone oxidoreductase core subunit S3 (NDUFS3, 459130, 1 : 1000), NADH:ubiquinone oxidoreductase subunit A9 (NDUFA9, 459100, 1 : 1000), mitochondrially encoded cytochrome *c* oxidase I (MTCO1/COX1, 459600, 1 : 1000), STAT5A (#13-3600, 1 : 1000), p-Tyr694-STAT5A (71-6900, 1 : 1000) from Invitrogen, Waltham, MA, USA; histone H3 (SAB4500352, 1 : 2000), Mitofusin 2 (MFN2, M6319, 1 : 1000) from Sigma-Aldrich; PPARγ coactivator 1 alpha (PGC1A, NBP1-04676, 1 : 1000) from Novus Biologicals, Littleton, CO, USA; BCL2-like protein 1 (BCLXL/BCL2L1, PA5-21676, 1 : 1000) from Thermo



Fisher Scientific and p-Thr202/Tyr204-ERK1/2 (675505, 1 : 1000) from BioLegend. Vimentin (fibroblast-specific protein) was used as loading control. In addition, naphthol blue (NB) membrane staining was performed to verify equal loading. Band densities were quantified with IMAGEJ software (Wayne Rasband, NIH, Kensington, MD, USA).

### Subcellular fractionation

Nuclear fraction was obtained with the Nuclei EZ Prep Nuclei Isolation kit (Sigma-Aldrich; NUC101) following supplier's instructions. Loading control for nuclear extracts was assessed by western blot detection of Histone H3.

### RNA extraction, reverse transcription and quantitative PCR

Total RNA was obtained with the RNeasy Mini Kit (Qiagen, Hilden, Germany) following the manufacturer's instructions. RNA concentration measurements, reverse transcription and quantitative real-time PCR were done as described [82,86]. The following ThermoFisher probes were used: *Bcl2* (Rn99999125\_m1) and *Nfe2l2* (Nrf2, Rn00582415\_m1). *Gapdh* (Rn01775763\_g1) was used as a loading control. The number of independent samples and replicates is specified in the figure legends.

### Cell culture immunofluorescence

Cells were cultured on glass coverslips and fixed with 4% paraformaldehyde (Sigma; P1213) for 20 min at room temperature, washed with PBS, blocked and permeabilized in PBS containing 5% FBS, 5% Horse serum (Gibco; 26050088) and 0.1% Triton X-100 (Sigma; T8787) before incubation with primary antibodies overnight at 4 °C and secondary antibodies for 1 h at RT. Antibodies used were: dihydrolipoamide dehydrogenase (DLD, ab133551, 1 : 250 from Abcam) and tubulin alpha 1a (TUBA1A, T5168, 1 : 1000 from Sigma-Aldrich). Secondary antibodies were coupled to Alexa Fluor 488 (Life Technologies, Carlsbad, CA, USA; A11034) or Alexa Fluor 594 (Life Technologies A11005). Hoechst 33342 (5 µg·mL<sup>-1</sup>) (Sigma; B2261) was included with the secondary antibodies mix to stain nuclei. Coverslips were mounted on Mowiol (Merck, Kenilworth, NJ, USA; 475904) and visualized using confocal microscopy (model FV1000; Olympus, Tokyo, Japan) with oil-immersion ×60 magnification objectives. Images were obtained with Fluoview FV1000 software (Olympus) and mitochondrial distribution was analyzed using IMAGEJ software.

### Tissue immunofluorescence

Freshly dissected hearts and lungs of adult male rats ( $n = 2$ , 10 months) were embedded in O.C.T. cryostat

medium and frozen in isopentane/liquid N<sub>2</sub>, as previously mentioned [87] (<https://doi.org/10.1113/jphysiol.2009.186577>). Four slices of 7 µm (for myocardial tissue) and 14 µm (for lung tissue) thick sections were cut with a cryostat (Leica CM 3050 S, Wetzlar, USA) and mounted in the same slide (one slice for each tissue). Samples were fixed during 10 min in formaldehyde 4% at RT, permeabilized (10 min incubation with 0.2% Tween 20/PBS at RT) and exposed to blocking buffer (BB, 5% FBS\_0.1% Tween 20/PBS) for 1 h at RT. Primary immunolabeling was performed overnight at 4 °C with rabbit anti-pSTAT3 (Tyr705; 1 : 100, #9145 Cell Signaling) and anti-vimentin (1 : 500 in BB, #ab45939; Abcam) antibodies. Secondary labeling was performed by 1 h incubation at RT with goat anti-rabbit IgG (H+L, Alexa Fluor 488, #A11008; Invitrogen) for p-STAT3 and direct conjugation with Alexa 594 using the Apex™ Antibody labeling kit (#A10474; Invitrogen) for vimentin. Cell nuclei were stained with 5 µg·mL<sup>-1</sup> Hoechst-33342 (#B2261 Sigma). Single z-planes (40× objective) were acquired with a spectral confocal microscope (Zeiss, Jena, Germany; LSM980 Airyscan) and fluorescence was quantified as mean gray value in background-subtracted 16-bit images (IMAGEJ).

### Statistical analysis

Statistics were performed with GRAPHPAD PRISM (GraphPad Software, San Diego, CA, USA), unless indicated otherwise. Two-way analysis of variance (ANOVA) was performed to compare differences in the experimental value means split in two independent variables (e.g., drug and ischemia) and for possible interaction, followed by Sidak's test to compare means between groups. One-way ANOVA was used to determine whether experimental value means were different when comparing three or more groups (e.g., between the three fibroblast types), provided that we had a high number of experimental replicates and/or that Brown–Forsythe test indicated no differences between standard deviations (SD). For multiple comparisons in experiments with low number of replicates in each category due to experimental constraints, or when experimental values were very sparse or with different SD, non-parametric Kruskal–Wallis test was selected, followed by *post-hoc* Dunn's test for pair-wise comparisons between groups or Dunnett's test for comparisons versus the control group (e.g., CF). Student's *t* test and non-parametric Mann–Whitney *U* test were performed when comparing means/medians in assays performed with two experimental groups. The exact statistical test performed in each experiment is indicated in the corresponding figure legend. The exact number of experiments, performed in duplicates, is specified in each figure legend. The  $P < 0.05$  level was selected as the point of minimal statistical significance in every comparison. Ns, not significant; \* $P < 0.05$ ; \*\* $P < 0.01$ ; \*\*\* $P < 0.001$  and \*\*\*\* $P < 0.0001$ .

## Acknowledgements

This research was funded by Ministerio de Ciencia e Innovación (MICINN), Gobierno de España, grant numbers SAF2013-44942-R and PID2019-104509RB-I00 to DS; Fundació La Marató TV3, grant number 20153810 to D.S; A.B. holds a contract from Fundació La Marató TV3 and IRBLleida/Diputació de Lleida; Generalitat de Catalunya, (AGAUR) grant number 2017SGR996 to DS; PP-G Laboratory support was obtained through research grants from MICINN (SAF2017/88275R) and CIBERONC (CB16/12/00334); JI and MR-M Laboratory support was obtained from Instituto de Salud Carlos III (ISCIII-FIS) grant PI19-01196; AZ Laboratory support was obtained through research grants from MICINN (PID2019-106209RB-I00), and the Generalitat de Catalunya, (AGAUR) grant number 2017SGR1015. AZ is a recipient of an ICREA 'Academia' Award (Generalitat de Catalunya). We gratefully acknowledge institutional funding from the MINECO through the Centres of Excellence Severo Ochoa Award, and from the CERCA Programme of the Generalitat de Catalunya.

## Conflict of interest

The authors declare no conflict of interest.

## Author contributions

DS and ML conceptualized the study; DS, ML, JGV, GL-L, MP-O, PP-G, JI, MR-M, and AZ contributed to methodology; AB, JGV, AI, GL-L, and CL investigated the study; all authors validated the study; AB, JGV, ML, and DS made formal analysis; PP-G, MP-O, AZ, and DS contributed to resources; DS with ML contributed to writing—original draft preparation; DS with the contributions of all authors contributed to writing—review and editing; ML and DS supervised the data; DS contributed to main project administration; PP-G, AZ, and DS acquired funding. All authors have read and agreed to the final version of the manuscript.

## Peer review

The peer review history for this article is available at <https://publons.com/publon/10.1111/febs.16283>.

## Data availability statement

All data are available in the main text or the [Supporting information](#).

## References

- Lindsey ML, Goshorn DK, Squires CE, Escobar GP, Hendrick JW, Mingoia JT, Sweterlitsch SE & Spinale FG (2005) Age-dependent changes in myocardial matrix metalloproteinase/tissue inhibitor of metalloproteinase profiles and fibroblast function. *Cardiovasc Res* **66**, 410–419.
- MacKenna D, Summerour SR & Villarreal FJ (2000) Role of mechanical factors in modulating cardiac fibroblast function and extracellular matrix synthesis. *Cardiovasc Res* **46**, 257–263.
- Spinale FG (2007) Myocardial matrix remodeling and the matrix metalloproteinases: influence on cardiac form and function. *Physiol Rev* **87**, 1285–1342.
- Ieda M, Tsuchihashi T, Ivey KN, Ross RS, Hong TT, Shaw RM & Srivastava D (2009) Cardiac fibroblasts regulate myocardial proliferation through  $\beta$ 1 integrin signaling. *Dev Cell* **16**, 233–244.
- Camelliti P, Green CR, LeGrice I & Kohl P (2004) Fibroblast network in rabbit sinoatrial node: structural and functional identification of homogeneous and heterogeneous cell coupling. *Circ Res* **94**, 828–835.
- Gaudesius G, Miragoli M, Thomas SP & Rohr S (2003) Coupling of cardiac electrical activity over extended distances by fibroblasts of cardiac origin. *Circ Res* **93**, 421–428.
- Porter KE & Turner NA (2009) Cardiac fibroblasts: at the heart of myocardial remodeling. *Pharmacol Ther* **123**, 255–278.
- Del Re DP, Amgalan D, Linkermann A, Liu Q & Kitis RN (2019) Fundamental mechanisms of regulated cell death and implications for heart disease. *Physiol Rev* **99**, 1765–1817.
- Ebinger MW, Krishnan S & Schuger CD (2005) Mechanisms of ventricular arrhythmias in heart failure. *Curr Heart Fail Rep* **2**, 111–117.
- Piek A, de Boer RA & Silljé HHW (2016) The fibrosis-cell death axis in heart failure. *Heart Fail Rev* **21**, 199–211.
- Gourdie RG, Dimmeler S & Kohl P (2016) Novel therapeutic strategies targeting fibroblasts and fibrosis in heart disease. *Nat Rev Drug Discov* **15**, 620–638.
- Goldsmith EC, Bradshaw AD, Zile MR & Spinale FG (2014) Myocardial fibroblast–matrix interactions and potential therapeutic targets. *J Mol Cell Cardiol* **70**, 92–99.
- Tallquist MD & Molkentin JD (2017) Redefining the identity of cardiac fibroblasts. *Nat Rev Cardiol* **14**, 484–491.
- Camelliti P, Borg TK & Kohl P (2005) Structural and functional characterisation of cardiac fibroblasts. *Cardiovasc Res* **65**, 40–51.
- Kanisicak O, Khalil H, Ivey MJ, Karch J, Maliken BD, Correll RN, Brody MJ, Lin SCJ, Aronow BJ, Tallquist

- MD *et al.* (2016) Genetic lineage tracing defines myofibroblast origin and function in the injured heart. *Nat Commun* **7**, 1–14.
- 16 Meilhac SM & Buckingham ME (2018) The deployment of cell lineages that form the mammalian heart. *Nat Rev Cardiol* **15**, 705–724.
- 17 Pinto AR, Ilinykh A, Ivey MJ, Kuwabara JT, D'Antoni ML, Debuque R, Chandran A, Wang L, Arora K, Rosenthal NA *et al.* (2016) Revisiting cardiac cellular composition. *Circ Res* **118**, 400–409.
- 18 Litviňuková M, Talavera-López C, Maatz H, Reichart D, Worth CL, Lindberg EL, Kanda M, Polanski K, Heinig M, Lee M *et al.* (2020) Cells of the adult human heart. *Nature* **588**, 466–472.
- 19 Krenning G, Zeisberg EM & Kalluri R (2010) The origin of fibroblasts and mechanism of cardiac fibrosis. *J Cell Physiol* **225**, 631–637.
- 20 Plikus MV, Wang X, Sinha S, Forte E, Thompson SM, Herzog EL, Driskell RR, Rosenthal N, Biernaskie J & Horsley V (2021) Fibroblasts: origins, definitions, and functions in health and disease. *Cell* **184**, 3852–3872.
- 21 Fu X, Khalil H, Kanisicak O, Boyer JG, Vagnozzi RJ, Maliken BD, Sargent MA, Prasad V, Valiente-Alandi I, Blaxall BC *et al.* (2018) Specialized fibroblast differentiated states underlie scar formation in the infarcted mouse heart. *J Clin Invest* **128**, 2127–2143.
- 22 Khalil H, Kanisicak O, Prasad V, Correll RN, Fu X, Schips T, Vagnozzi RJ, Liu R, Huynh T, Lee S *et al.* (2017) Underlies cardiac fibrosis. *J Clin Invest* **127**, 3770–3783.
- 23 Khalil H, Kanisicak O, Vagnozzi RJ, Johansen AK, Maliken BD, Prasad V, Boyer JG, Brody MJ, Schips T, Kilian KK *et al.* (2019) Cell-specific ablation of Hsp47 defines the collagen-producing cells in the injured heart. *JCI Insight* **4**, e128722.
- 24 Chen H, Jing XY, Shen YJ, Wang TL, Ou C, Lu SF, Cai Y, Li Q, Chen X, Ding YJ *et al.* (2018) Stat5-dependent cardioprotection in late remote ischaemia preconditioning. *Cardiovasc Res* **114**, 679–689.
- 25 Burke RM, Burgos Villar KN & Small EM (2021) Fibroblast contributions to ischemic cardiac remodeling. *Cell Signal* **77**, 109824.
- 26 Brand CS, Lighthouse JK & Trembley MA (2019) Protective transcriptional mechanisms in cardiomyocytes and cardiac fibroblasts. *J Mol Cell Cardiol* **132**, 1–12.
- 27 Rossello X & Yellon DM (2018) The RISK pathway and beyond. *Basic Res Cardiol* **113**, 1–5.
- 28 Mayorga M, Bahi N, Ballester M, Comella JX & Sanchis D (2004) Bcl-2 is a key factor for cardiac fibroblast resistance to programmed cell death. *J Biol Chem* **279**, 34882–34889.
- 29 Puente BN, Kimura W, Muralidhar SA, Moon J, Amatruda JF, Phelps KL, Grinsfelder D, Rothermel BA, Chen R, Garcia JA *et al.* (2014) The oxygen-rich postnatal environment induces cardiomyocyte cell-cycle arrest through DNA damage response. *Cell* **157**, 565–579.
- 30 Kimura W, Muralidhar S, Canseco DC, Puente B, Zhang CC, Xiao F, Abderrahman YH & Sadek HA (2014) Redox signaling in cardiac renewal. *Antioxid Redox Signal* **21**, 1660–1673.
- 31 Blasco N, Cámara Y, Núñez E, Beà A, Barés G, Forné C, Ruíz-Meana M, Girón C, Barba I, García-Arumí E *et al.* (2018) Cardiomyocyte hypertrophy induced by endonuclease G deficiency requires reactive oxygen radicals accumulation and is inhibitable by the micropeptide humanin. *Redox Biol* **16**, 146–156.
- 32 Chouchani ET, Pell VR, James AM, Work LM, Saeb-Parsy K, Frezza C, Krieg T & Murphy MP (2016) A unifying mechanism for mitochondrial superoxide production during ischemia-reperfusion injury. *Cell Metab* **23**, 254–263.
- 33 Murphy E & Steenbergen C (2008) Mechanisms underlying acute protection from cardiac ischemia-reperfusion injury. *Physiol Rev* **88**, 581–609.
- 34 Murphy MP (2009) How mitochondria produce reactive oxygen species. *Biochem J* **417**, 1–13.
- 35 Ortiz-Prado E, Dunn JF, Vasconez J, Castillo D & Viscor G (2019) Partial pressure of oxygen in the human body: a general review. *Am J Blood Res* **9**, 1–14.
- 36 Carreau A, El H-R, Matejuk A, Grillon C & Kieda C (2011) Why is the partial oxygen pressure of human tissues a crucial parameter? Small molecules and hypoxia. *J Cell Mol Med* **15**, 1239–1253.
- 37 Pflieger J, He M & Abdellatif M (2015) Mitochondrial complex II is a source of the reserve respiratory capacity that is regulated by metabolic sensors and promotes cell survival. *Cell Death Dis* **6**, 1–14.
- 38 Chen ZX & Pervaiz S (2007) Bcl-2 induces pro-oxidant state by engaging mitochondrial respiration in tumor cells. *Cell Death Differ* **14**, 1617–1627.
- 39 Low ICC, Chen ZX & Pervaiz S (2010) Bcl-2 modulates resveratrol-induced ROS production by regulating mitochondrial respiration in tumor cells. *Antioxid Redox Signal* **13**, 807–819.
- 40 Molina AJA, Wikstrom JD, Stiles L, Las G, Mohamed H, Elorza A, Walzer G, Twig G, Katz S, Corkey BE *et al.* (2009) Mitochondrial networking protects  $\beta$ -cells from nutrient-induced apoptosis. *Diabetes* **58**, 2303–2315.
- 41 Schrepfer E & Scorrano L (2016) Mitofusins, from mitochondria to metabolism. *Mol Cell* **61**, 683–694.
- 42 Khacho M, Clark A, Svoboda DS, Azzi J, MacLaurin JG, Meghaizel C, Sesaki H, Lagace DC, Germain M, Harper ME *et al.* (2016) Mitochondrial dynamics impacts stem cell identity and fate decisions by regulating a nuclear transcriptional program. *Cell Stem Cell* **19**, 232–247.
- 43 Wu Z, Puigserver P, Andersson U, Zhang C, Adelmant G, Mootha V, Troy A, Cinti S, Lowell B, Scarpulla RC

- et al.* (1999) Mechanisms controlling mitochondrial biogenesis and respiration through the thermogenic coactivator PGC-1. *Cell* **98**, 115–124.
- 44 Soriano FX, Liesa M, Bach D, Chan DC, Palacín M & Zorzano A (2006) Evidence for a mitochondrial regulatory pathway defined by peroxisome proliferator-activated receptor- $\gamma$  coactivator-1 $\alpha$ , estrogen-related receptor- $\alpha$ , and mitofusin 2. *Diabetes* **55**, 1783–1791.
- 45 Wikstrom JD, Mahdavian K, Liesa M, Sereda SB, Si Y, Las G, Twig G, Petrovic N, Zingaretti C, Graham A *et al.* (2014) Hormone-induced mitochondrial fission is utilized by brown adipocytes as an amplification pathway for energy expenditure. *EMBO J* **33**, 418–436.
- 46 Chen Q, Hoppel CL & Lesnefsky EJ (2006) Blockade of electron transport before cardiac ischemia with the reversible inhibitor amobarbital protects rat heart mitochondria. *J Pharmacol Exp Ther* **316**, 200–207.
- 47 Chouchani ET, Pell VR, Gaude E, Aksentijević D, Sundier SY, Robb EL, Logan A, Nadtochiy SM, Ord ENJ, Smith AC *et al.* (2014) Ischaemic accumulation of succinate controls reperfusion injury through mitochondrial ROS. *Nature* **515**, 431–435.
- 48 Semenza GL (2014) Hypoxia-inducible factor 1 and cardiovascular disease. *Annu Rev Physiol* **76**, 39–56.
- 49 Zang H, Mathew RO & Cui T (2020) The dark side of Nrf2 in the heart. *Front Physiol* **11**, 1–8.
- 50 Nitire SK & Jaiswal AK (2012) Nrf2 protein up-regulates antiapoptotic protein Bcl-2 and prevents cellular apoptosis. *J Biol Chem* **287**, 9873–9886.
- 51 Krylatov AV, Maslov LN, Voronkov NS, Boshchenko AA, Popov SV, Gomez L, Wang H, Jaggi AS & Downey JM (2018) Reactive oxygen species as intracellular signaling molecules in the cardiovascular system. *Curr Cardiol Rev* **14**, 290–300.
- 52 Yeramian A, Santacana M, Sorolla A, Llobet D, Encinas M, Velasco A, Bahi N, Eritja N, Domingo M, Oliva E *et al.* (2011) Nuclear factor-B2/p100 promotes endometrial carcinoma cell survival under hypoxia in a HIF-1 $\alpha$  independent manner. *Lab Invest* **91**, 859–871.
- 53 Hadebe N, Cour M & Lecour S (2018) The SAFE pathway for cardioprotection: is this a promising target? *Basic Res Cardiol* **113**, 9.
- 54 Fukada T, Hibi M, Yamanaka Y, Takahashi-Tezuka M, Fujitani Y, Yamaguchi T, Nakajima K & Hirano T (1996) Two signals are necessary for cell proliferation induced by a cytokine receptor gp130: Involvement of STAT3 in anti-apoptosis. *Immunity* **5**, 449–460.
- 55 Nielsen M, Kæstel CG, Eriksen KW, Woetmann A, Stokkedal T, Kaltoft K, Geisler C, Röpke C & Ødum N (1999) Inhibition of constitutively activated Stat3 correlates with altered Bcl-2/Bax expression and induction of apoptosis in mycosis fungoides tumor cells. *Leukemia* **13**, 735–738.
- 56 Stephanou A & Latchman DS (2005) Opposing actions of STAT-1 and STAT-3. *Growth Factors* **23**, 177–182.
- 57 Haga S, Terui K, Zhang HQ, Enosawa S, Ogawa W, Inoue H, Okuyama T, Takeda K, Akira S, Ogino T *et al.* (2003) Stat3 protects against Fas-induced liver injury by redox-dependent and -independent mechanisms. *J Clin Invest* **112**, 989–998.
- 58 Bhattacharya S, Ray RM & Johnson LR (2005) STAT3-mediated transcription of Bcl-2, Mcl-1 and C-IAP2 prevents apoptosis in polyamine-depleted cells. *Biochem J* **392**, 335–344.
- 59 Sepúlveda P, Encabo A, Carbonell-Uberos F & Miñana MD (2007) BCL-2 expression is mainly regulated by JAK/STAT3 pathway in human CD34+ hematopoietic cells. *Cell Death Differ* **14**, 378–380.
- 60 Wegrzyn J, Potla R, Chwae YJ, Sepuri NBV, Zhang Q, Koeck T, Derecka M, Szczepanek K, Szlag M, Gornicka A *et al.* (2009) Function of mitochondrial Stat3 in cellular respiration. *Science* **323**, 793–797.
- 61 Carbognin E, Betto RM, Soriano ME, Smith AG & Martello G (2016) Stat3 promotes mitochondrial transcription and oxidative respiration during maintenance and induction of naive pluripotency. *EMBO J* **35**, 618–634.
- 62 Zouein FA, Duhé RJ, Arany I, Shirey K, Hosler JP, Liu H, Saad I, Kurdi M & Booz GW (2014) Loss of STAT3 in mouse embryonic fibroblasts reveals its Janus-like actions on mitochondrial function and cell viability. *Cytokine* **66**, 7–16.
- 63 Terui K, Enosawa S, Haga S, Zhang HQ, Kuroda H, Kouchi K, Matsunaga T, Yoshida H, Engelhardt JF, Irani K *et al.* (2004) Stat3 confers resistance against hypoxia/reoxygenation-induced oxidative injury in hepatocytes through upregulation of Mn-SOD. *J Hepatol* **41**, 957–965.
- 64 Negoro S, Kunisada K, Fujio Y, Funamoto M, Darville MI, Eizirik DL, Osugi T, Izumi M, Oshima Y, Nakaoka Y *et al.* (2001) Activation of signal transducer and activator of transcription 3 protects cardiomyocytes from hypoxia/reoxygenation-induced oxidative stress through the upregulation of manganese superoxide dismutase. *Circulation* **104**, 979–981.
- 65 Verdura S, Cuyàs E, Llorach-Parés L, Pérez-Sánchez A, Micol V, Nonell-Canals A, Joven J, Valiente M, Sánchez-Martínez M, Bosch-Barrera J *et al.* (2018) Silibinin is a direct inhibitor of STAT3. *Food Chem Toxicol* **116**, 161–172.
- 66 Nagata Y & Todokoro K (1995) Thrombopoietin induces activation of at least two distinct signaling pathways. *FEBS Lett* **377**, 497–501.
- 67 Rane SG & Reddy EP (2000) Janus kinases: components of multiple signaling pathways. *Oncogene* **19**, 5662–5679.
- 68 Meydan N, Grunberger T, Dadi H, Shahar M, Arpaia E, Lapidot Z, Leeder JS, Freedman M, Cohen A, Gazit A *et al.* (1996) Inhibition of acute lymphoblastic leukaemia by a Jak-2 inhibitor. *Nature* **379**, 645–648.



- 69 Furtado MB, Costa MW, Pranoto EA, Salimova E, Pinto AR, Lam NT, Park A, Snider P, Chandran A, Harvey RP *et al.* (2014) Cardiogenic genes expressed in cardiac fibroblasts contribute to heart development and repair. *Circ Res* **114**, 1422–1434.
- 70 Hafstad AD, Nabeebaccus AA & Shah AM (2013) Novel aspects of ROS signalling in heart failure. *Basic Res Cardiol* **108**, 359.
- 71 DeBerardinis RJ & Chandel NS (2016) Fundamentals of cancer metabolism. *Sci Adv* **2**, e1600200.
- 72 Kasahara A, Cipolat S, Chen Y, Dorn GW 2nd & Scorrano L (2013) Mitochondrial fusion directs cardiomyocyte differentiation via calcineurin and Notch signaling. *Science* **342**, 734–737.
- 73 Sprenger H-G & Langer T (2019) The good and the bad of mitochondrial breakups. *Trends Cell Biol* **29**, 888–900.
- 74 Chen H, Detmer SA, Ewald AJ, Griffin EE, Fraser SE & Chan DC (2003) Mitofusins Mfn1 and Mfn2 coordinately regulate mitochondrial fusion and are essential for embryonic development. *J Cell Biol* **160**, 189–200.
- 75 Muñoz JP, Ivanova S, Sánchez-Wandelmer J, Martínez-Cristóbal P, Noguera E, Sancho A, Díaz-Ramos A, Hernández-Alvarez MI, Sebastián D, Mauvezin C *et al.* (2013) Mfn2 modulates the UPR and mitochondrial function via repression of PERK. *EMBO J* **32**, 2348–2361.
- 76 Papanicolaou KN, Khairallah RJ, Ngoh GA, Chikando A, Luptak I, O'Shea KM, Riley DD, Lugus JJ, Colucci WS, Lederer WJ *et al.* (2011) Mitofusin-2 maintains mitochondrial structure and contributes to stress-induced permeability transition in cardiac myocytes. *Mol Cell Biol* **31**, 1309–1328.
- 77 Hall AR, Burke N, Dongworth RK, Kalkhoran SB, Dyson A, Vicencio JM, Dorn GWII, Yellon DM & Hausenloy DJ (2016) Hearts deficient in both Mfn1 and Mfn2 are protected against acute myocardial infarction. *Cell Death Dis* **7**, e2238.
- 78 Lee H, Herrmann A, Deng JH, Kujawski M, Niu G, Li Z, Forman S, Jove R, Pardoll DM & Yu H (2009) Persistently activated Stat3 maintains constitutive NF- $\kappa$ B activity in tumors. *Cancer Cell* **15**, 283–293.
- 79 Dawson MA, Bannister AJ, Saunders L, Wahab O-A, Liu F, Nimer SD, Levine RL, Göttgens B, Kouzarides T & Green AR (2011) Nuclear JAK2. *Blood* **118**, 6987–6988.
- 80 Girodon F, Steinkamp MP, Cleyrat C, Hermouet S & Wilson BS (2011) Confocal imaging studies cast doubt on nuclear localization of JAK2V617F. *Blood* **118**, 2633–2634.
- 81 Sanchis D, Mayorga M, Ballester M & Comella JX (2003) Lack of Apaf-1 expression confers resistance to cytochrome c-driven apoptosis in cardiomyocytes. *Cell Death Differ* **10**, 977–986.
- 82 Bahi N, Zhang JS, Llovera M, Ballester M, Comella JX & Sanchis D (2006) Switch from caspase-dependent to caspase-independent death during heart development – essential role of endonuclease G in ischemia-induced DNA processing of differentiated cardiomyocytes. *J Biol Chem* **281**, 22943–22952.
- 83 Zhang JS, Ye JM, Altafaj A, Cardona M, Bahi N, Llovera M, Canas X, Cook SA, Comella JX & Sanchis D (2011) EndoG links Bnip3-induced mitochondrial damage and caspase-independent DNA fragmentation in ischemic cardiomyocytes. *PLoS One* **6**, e17998.
- 84 Blasco N, Beà A, Barés G, Girón C, Navaridas R, Irazoki A, López-Lluch G, Zorzano A, Dolcet X, Llovera M *et al.* (2020) Involvement of the mitochondrial nuclease EndoG in the regulation of cell proliferation through the control of reactive oxygen species. *Redox Biol* **37**, 101736.
- 85 Rodríguez-Aguilera J, Cortés A, Fernández-Ayala D & Navas P (2017) Biochemical assessment of coenzyme Q10 deficiency. *J Clin Med* **6**, 27.
- 86 Cardona M, López JA, Serafín A, Rongvaux A, Inserte J, García-Dorado D, Flavell R, Llovera M, Cañas X, Vázquez J *et al.* (2015) Executioner caspase-3 and 7 deficiency reduces myocyte number in the developing mouse heart. *PLoS One* **10**, e0131411.
- 87 Rodríguez-Sinovas A, Sánchez JA, González-Loyola A, Barba I, Morente M, Aguilar R, Agulló E, Miró-Casas E, Esquerda N, Ruiz-Meana M *et al.* (2010) Effects of substitution of Cx43 by Cx32 on myocardial energy metabolism, tolerance to ischaemia and preconditioning protection. *J Physiol* **588**, 1139–1151.

## Supporting information

Additional supporting information may be found online in the Supporting Information section at the end of the article.

**Fig. S1.** Microarray expression data mining of human cultured fibroblasts and protein expression in cultured adult rat fibroblasts.

**Fig. S2.** Comparative expression of OxPhos genes in human and rat fibroblasts.

**Fig. S3.** Complementary data on oxygen consumption and ETC complex protein expression in neonatal fibroblasts.

**Fig. S4.** Analysis of respiration in rat cardiac fibroblasts expressing normal and low levels of BCL2.

**Fig. S5.** Expression of proteins involved in mitochondrial dynamics in rat neonatal fibroblast cultures.

**Fig. S6.** Analysis of the expression and phosphorylation of MAPK ERK1/2, AKT, HIF1A, NRF2 and RELA/p65 (NF $\kappa$ B) in neonatal rat fibroblasts.

**Fig. S7.** Status of the Molecular Signatures Database gene sets STAT3 and STAT5 in cultured human fibroblasts.

**Fig. S8.** Immunodetection of p-Tyr705-STAT3 on heart and lung tissue from adult rats and effects of

Silibinin (SBN) treatment on rat neonatal cardiac, pulmonary and dermal fibroblasts.

**Fig. S9.** Effects of STAT5 inhibition and analysis of the combination of STAT3 and STAT5 inhibition in pulmonary and dermal fibroblasts, and protein

expression, respiration and ROS production in rat neonatal cardiac fibroblasts.

**Fig. S10.** Effects of JAK2 inhibition in survival of pulmonary and dermal fibroblasts, and respiration and protein expression of rat neonatal cardiac fibroblasts.